We thank the reviewers for the time they took and for the very helpful comments provided, which will help us to improve the manuscript. A pointwise reply to the reviewer's comment is given below.

Reviewer #1:

1.) *Equations 3, 4 and 8-10, give a diagnostic value of the 5 variables, given a forcing field of temperature and humidity. These are not prognostic equations, they don't give a time evolution, despite what said in section 2.1. This is ok, but then why are figures 1 to 5 "monthly means": they would each show field diagnosed from the forcing fields specified in section 3. There is a time evolution for the transient kinetic energy u and v and of the momentum flux, <v'u'>, indeed, so I don't understand how these articulate with the diagnostic equations. Is the above correct*?

Yes, Eqs. 3, 4, 8 - 10 are not prognostic equations. They describe how the state of the model is calculated from the input data (surface temperature, humidity, and cumulus cloud amount). The input data is given as monthly mean data, therefore figures 1 to 5 show the mean state of the model for a given month.
The transient kinetic equations are also diagnostic equations and the completely derivation of the diagnostic equations has been described in Coumou et al. (2011).

We have rewritten the manuscript to state this more clearly (p .4, l. 12-21, p. 7,l. 1-4).

2.) *In fact the 2D equations of Petoukhov et al (2000) for temperature and humidity are prognostic equations, but they are just mentioned at the beginning. Are you integrating these equations along with the equations of the kinetic energies? This is not what it seems to be implied at page 6 line 5. And also, if so, how does forcing comes in?*

No, we are not integrating the equations for temperature and humidity.
The scope of this study is to describe and test a new set of equations of the dynamical core only. The prognostic equations for T and humidity and the diagnostic equations for EKE have been described and validated in previous work (notably Petoukhov et al, 2000 and Coumou et al, 2011).

Therefore, in order to make the manuscript not larger than needed, we prefer to only reference those publications, rather than providing the full derivation again.

We rewrote this part to make it clearer (p. 3, l. 24-30; p. 4, l. 12-21; p. 7,l. 1-4; p. 7, l. 14 – p. 8, l. 4).

3.) *As you see these are all very basic doubts that clearly come from a bad structuring of the paper. Note also that the supplementary material is not well articulated with the text. The text should contain enough information to understand the basics (like my doubts above). As for now, the derivation of the equations are divided in the two parts -test and supplement - in a chaotic way. Also note that a section 2 of sup. material is referenced in the text, but it's not in there*

We agree with the reviewer that we did not sufficiently explain our approach. Therefore we have rewritten the main text such that it has enough information to understand our general approach and also better link it to information in the Suppl. Information.

We have described the model setup and the experiment in more detail and also have explained already in the abstract the novelty of our model (p. 1, l.21 – p.2, l. 2; p.3, l. 24 – 36; p. 4, l.12 - 21).
In addition, we added Suppl. Mat. 2 (in Suppl. Inf.: now S1.3 Zeroth order solution of the thermally induced waves of the barotropic vorticity equation at the EBL; p.2, l. 7 - p.3,l. 8).

4.) *In addition to the clarity problem, which is in itself bad enough to require a major revision of the article, there is another point that is not clear to me. The Aeolus model as it is presented has already been published in Coumou et al 2011. Is the coupling with the convection model , or the coupling with the temperature and humidity 2D equations of Petoukhov et al (2000) the novelty? Is it the optimization of parameters? Please state this clearly. I have to say that the optimization does not appear to have such a major impact to me.*

From a theoretical point of view, the novelty is the newly derived statistical dynamical equations of the large-scale zonal-mean field and the planetary waves, and their embedding in the model's dynamical core.

From a technical point of view, we present a detailed parameter-optimization scheme to validate the dynamical core against observations. This is also presented the first time.

5.) *Note also that the method of optimization (simulated annealing) should at least be schematically described.*

We provided the following schematic plot of the optimization process in the Suppl. Mat. as well as an additional reference in the main text (Kirkpatrick, 1984) (in Suppl. Inf.: p. 6, l. 10).

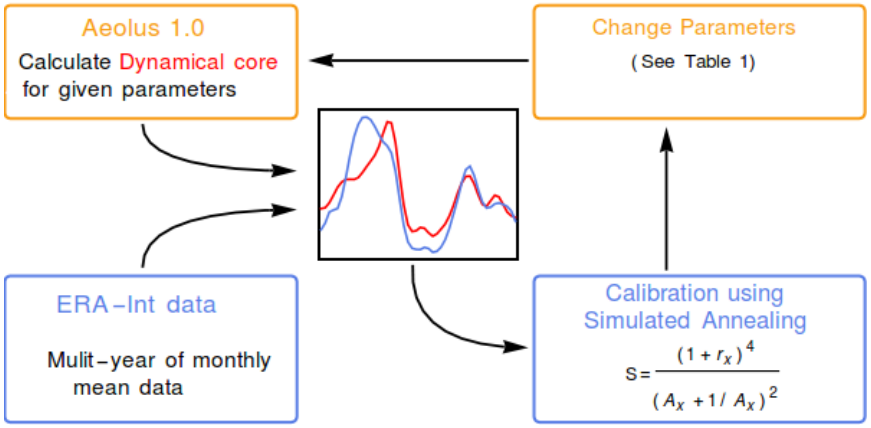

Figure 1 Schematic plot of the optimization process: The dynamical core is calculated for given parameters (presented in Table 1). In order to find the optimized parameters, we calibrate the dynamical core with Simulated Annealing and using ERA-Int data to construct the skill function.

6.) *page 2 line 32 "convective plus 3 layer stratiform" What does this mean?*

It means, that our cloud model simulates 3 types of stratiform clouds, at low-level, mid-level, and upper-level (as described in detail in Eliseev et al, 2013).

The fourth cloud type represents convective (cumulus) clouds. In the equations for the dynamical core, only cumulus clouds are considered. We clarified this in the text. (p.3, l. 38-p. 4, l. 2)

7.) *Section S1.2 "With K_z = 005 and In (4)" incomprehensible*

We changed that sentence to: With $K_z = 0.005\ z$ and

$$A = \frac{\mathcal{L}\overline{\langle P_{co}\rangle}}{H_0}\frac{\overline{\langle u_{sf}\rangle}}{\Gamma_a - \Gamma_0 - \Gamma_1(T_a - T_0)\left(1 - a_q q_s^2\right) + \Gamma_2 n_c}$$

(in Suppl. Information, p. 3, l. 11 - 13)

8.) *Supp. mat. at the bottom. Is the independency of the large scale and synoptic waves a reasonable assumption? Comment.*

This sentence was phrased incorrectly. Large scale und synoptic waves are not independent.
Due to a "gap" in the three-dimensional (period-wavelength-phase velocity) spectrum of atmospheric processes (see, e.g., Fraedrich & Böttger 1978, Coumou et al. 2011), the interaction of the synoptic-scale wind component with the large scale long-term wind component (on time scales of about 10-20 days and longer) could to a first approximation, be represented in terms of its ensemble (statistical) characteristics (the second and higher-order moments), and not in terms of the individual eddies (Saltzman, 1978).
Because of this gap between the two spectra, it can be assumed that the long-term component is nearly constant over synoptic timescales.
Hence, the equation can be written as:
<xy'>=x<y'>=x*0=0, again this is explained in detail in Coumou et al. 2011.

We rewrote this part to make it clearer (in Suppl. Information, p. 5, l. 5 - 13).

9.) *Repetition page 4 sup mat. Paragraph "The contribution to the vertical…"*

We removed the repetition.

10.) *Page 4 of Supp. Mat. The scale analysis attests,have you done the scale analysis,or is taken from literature?*

This scaling analysis is described in:
Petoukhov V, Ganopolski A, Claussen M (2003) POTSDAM - a set of atmosphere statistical-dynamical models: theoretical background. Potsdam-Institut für Klimafolgenforschung, ISSN 1436-0179, 136 pp, http://www.pikpotsdam.de/research/publications/pikreports/.files/pr81.pdf

Using the magnitude analysis

$$\langle\overline{w}\rangle\frac{\partial\langle u\rangle}{\partial z} = H^*\left(\frac{u^*}{L^*}\right)\left(\frac{\langle u\rangle}{H}\right) \ll 1$$

where
H = 10^4m is the atmospheric density vertical scale,
u* =10 m/s is characteristic scales of the planetary wave velocities

L*= 3*10^6 are the characteristic scales of planetary horizontal lengths, and H*=H Ro*, where Ro*=u*/(L*f) is the Rossby number for the planetary waves.

11.) Page 3, eq.3, could we call it geostrophic and thermal wind balance?

Yes, it could be called thermal wind balance, we added a sentence in the manuscript (p. 4, l. 31).

12.) Page 3, formula for the meridional pressure, where does that come from? Please describe it more carefully.

It is derived from Petoukhov et al. (2000) eq. (13). In order to make the manuscript not larger than needed, we would like to only reference those equations, derived in other publications rather describe them again (p. 5, l. 3).

13.) page 3 line 9 "Supl.Ment"

We rewrote as suggested.

14.) Page 3 line 25 repetition, reword.

We removed the repetition.

15.) page 4 line 5. In fact the parameters gamma and a_q are not at all explained in the table. just listed along with their value.

Gamma is the lapse rate equation, which is assumed to be linear (Petoukhov et al, 2000):

$$\Gamma = \Gamma_0 + \Gamma_1(\mathrm{T_a} - \mathrm{T_0})\left(1 - \mathrm{a_q q_s^2}\right) - \Gamma_2 \mathrm{n_c}$$

We added this in the manuscript (p. 6, l. 14).
The parameters are all described in Table 1.

16.) pag 4 line7 is n_c constant or is it computed? If it is a constant, what's it value?

We used observational data: Multi-year averages of monthly mean, El Niño and La Niña months cumulative cloud fraction is taken from ISSCP (Rossow and Schiffer, 1999). We added a sentence in the manuscript to make that clearer (p. 5, l. 15-16; p. 8, l. 13 - 15).

17.) pag 4 line 9, is U_sf the same as U_Sprofile in the supplementary material? if so, it is not clearly explained, what does "The additional calculating of U_sprofile instead of using the calculated surface zonal velocity is done to avoid instabilities." mean?

Yes, U_sf is the same as Us_profile. We will rewrite that in the manuscript (p. 5, l. 17; in Suppl. Inf.: p. 4, l. 1 - 5).
Instabilities can emerge due to the strong positive feedback between the meridional temperature profile, surface winds and vertical wind velocity, which can lead to high latent heat release (moisture-convection feedback) (Grabowski and Moncrieff, 2004). In nature these would be damped out but due to the fixed troposphere height in the model, we have to parameterize it.

18.) *Page 4 last line. There is no S.2 in the supplementary material*

We included Suppl. Inf. 2 (in Suppl. Inf.: S1.3 p. 2, l. 7 - p. 3,l. 6)..

19.) page 5 line 19 “equipartitioned

We rewrote it (p. 7, l. 6).

20.) *in the supplementary material, the explanation of eq.4 is not complete, it is not shown why the introduction of coefficients d1 d2 and d3 is necessary and how they are chosen*

The derived equation for the meridional velocity does not account for latent heat release associated with convective precipitation. To capture this additional term we include convective precipitation and finally introduce tuning parameters, which have values close to 1.
We added that part to explain it better (in Suppl. Inf. p. 6, l. 5 - 7).

21.) *Page 4 last line. There is no S.2 in the supplementary material*

We included Suppl. Inf. 2 (in Suppl. Inf.: S1.3 p. 2, l. 7 - p. 3,l. 8)..

22.) *Note also that the supplementary material is not references, page numbers, line numbers*

We changed that in the updated manuscript.

Reviewer #2:

1.) *While reviewing this article I have looked through both the comments of the other reviewer and the authors’ response. I agree with almost all of the other reviewer’s comments and I am pleased to see that the authors have responded with changes to their manuscript. For this reason I will try to not repeat comments made in the other review that have already been addressed. I think that the material within this article is good, however I found it difficult to read and some parts hard to understand. As a general point, I think the authors should take time to try and make the article more accessible. Below are a few more specific comments*.

Thanks, we rewrote those parts in order to make the article more accessible as outlined below.

2.) *I think that the introduction needs more information about statistical dynamical atmosphere models. For readers from a dynamical core background it would be very useful to give a brief paragraph about how they work and the key differences to dynamical cores.*

We agree with the reviewer and included the following information about SDAMs (p. 3, l. 4 - 23):

In particular, statistical-dynamical (SD) atmosphere models parameterize smaller scale (and more short-lived) processes like synoptic eddy activity in terms of the large-scale, long-term fields. The assumption of those models is thus that atmospheric variables can be expressed in separate terms of a large-scale, long-term component, with characteristic spatial and temporal scales of L>1000 km and T>10 days, and a small-scale component like ensembles of synoptic-scale eddies and waves. The latter are then parameterized by their averaged statistical

characteristics (e.g. their total kinetic energy and heat, moist and momentum fluxes). This means that transport effects of the fast moving weather systems on the large-scale, long-term atmospheric motion are averaged (Ehlers et al., 2001).
The essential difference to GCMs is thus the point of truncation in the frequency spectrum of atmospheric motion (Saltzman, 1978). GCMs solve all phenomena of frequencies lower than and including synoptic cyclones (and sometimes even mesoscale systems), whereas SD models parameterize all scales smaller and equal to synoptic. Much of the difficulty in SD models is to define physically reasonable parameterizations occurring in the equations (Saltzman, 1978). For Aeolus the synoptic parameterization has been described in detail in Coumou et al. (2011).
As written above, SD models are also spatially averaged since for long-term climate simulations, we are typically interested in the large spatial aspects of the climate. It is further practical to split the large-scale, long-term field into two components: the zonally averaged mean field, and the asymmetric departure of the field from the zonally averaged fields characterizing the East-West variations. The azonal variables can be, for example, resolved by 1-dimensional Fourier components around latitude circles or into spherical harmonics (Saltzman, 1978).

3.) *The introduction should also better explain the aims of the paper. This is covered briefly in the abstract, but it would be worth including this in the introduction. The way the article is worded it is not clear if the work presented is a completely new model, or something coupled to an existing model (which is what I think is the case). This needs to be clarified.*

We agree with the reviewer and will include the aims of this paper in the introduction as well. In addition, we explain the model and the new aspects in more detail. In particular, we wrote (p. 3, l. 24 - 36):

Here, we present the Aeolus 1.0 dynamical core, developed at the Potsdam Institute for Climate Impact Research (PIK), a new SD model for the atmosphere. It uses some aspects of the atmosphere module of the EMIC CLIMBER-2 developed by Petoukhov et al. (2000). The dynamical core is completely new with novel equations for the large-scale meridional wind speed as well as quasi-stationary planetary waves. Together with the synoptic parameterizations presented in Coumou (2011), these equations form the new dynamical core of Aeolus 1.0. The model is coupled with the cloud module consisting of a three-layer stratiform cloud plus convective cloud scheme as presented and validated in Eliseev et al. (2013).
Further, we present the equations of the model and validate the dynamical core using a parameter optimization experiment. Aeolus 1.0 is forced with prescribed surface temperature, surface humidity and cumulus cloud fraction to test the model's performance. In particular we examine the reproduction of the seasonal cycle, and the influence of ENSO of our model and compare relevant dynamical fields of the model output against seasonal means of ERA-Interim reanalysis data (climatology 1983-2009). The effects of parameter tuning are evaluated to improve the performance of the model.

4.) *Page 8, line 7, you exclude the polar regions. I am curious why it is poleward of 60 degrees for SH but 70 degrees for NH. Why the difference?*

We wanted to exclude influences of the Antarctica, which is located at south of 60 degrees. The reanalysis data is spikey over Antarctica. We wrote this in the revised manuscript (p. 9, l. 25-26).

5.) *In the abstract, page 1 line 18, change "enables us to do climate simulations" to "enables us to perform climate simulations*

Thanks, we corrected it (p. 1, l. 18).

6.) *Typo, page 7 line 29. Full stop needed after the reference.*

Thanks, we corrected it (p. 9, l. 12).

References

Claussen, M., Mysak, L., Weaver, A., Crucifix, M., Fichefet, T., Loutre, M. F., Weber, S., Alcamo, J., Alexeev, V., Berger, A., Calov, R., Ganopolski, A., Goosse, H., Lohmann, G., Lunkeit, F., Mokhov, I., Petoukhov, V., Stone, P. and Wang, Z.: Earth system models of intermediate complexity: Closing the gap in the spectrum of climate system models, Clim. Dyn., 18(7), 579–586, doi:10.1007/s00382-001-0200-1, 2002.

Coumou, D., Petoukhov, V. and Eliseev, A. V.: Three-dimensional parameterizations of the synoptic scale kinetic energy and momentum flux in the Earth's atmosphere, Nonlinear Process. Geophys., 18(6), 807–827, doi:10.5194/npg-18-807-2011, 2011.

Ehlers, E., Krafft, T. and (Eds.): Understanding the Earth System: Compartments, Processes and Interactions, Springer-Verlag, Berlin, Heidelberg, 2001.

Eliseev, A. V., Coumou, D., Chernokulsky, A. V., Petoukhov, V. and Petri, S.: Scheme for calculation of multi-layer cloudiness and precipitation for climate models of intermediate complexity, Geosci. Model Dev., 6(5), 1745–1765, doi:10.5194/gmd-6-1745-2013, 2013.

Grabowski, W. W. and Moncrieff, M. W.: Moisture–convection feedback in the tropics, Q. J. R. Meteorol. Soc., 130(604), 3081–3104, doi:10.1256/qj.03.135, 2004.

Kirkpatrick, S.: Optimization by simulated annealing: Quantitative studies, J. Stat. Phys., 34, 975–986, doi:10.1007/BF01009452, 1984.

McGuffie, K. and Henderson-Sellers, A.: A Climate Modelling Primer, 3rd ed., edited by J. Wiley and Sons, 2005.

Petoukhov, V., Ganopolski, A., Brovkin, V., Claussen, M., Eliseev, A. V., Kubatzki, C. and Rahmstorf, S.: CLIMBER 2: a climate system model of intermediate complexity. Part I: model description and performance for present climate, Clim. Dyn., 16, 1–17, doi:10.1007/PL00007919, 2000.

Rossow, W. B. and Schiffer, R. a: Advances in Understandig Clouds from ISCCP, Bull. Amer. Meteor. Soc., 80(11), 2261–2287, doi:10.1175/1520-0477(1999)080<2261:AIUCFI>2.0.CO;2, 1999.

Saltzman, B.: A Survey of Statistical-Dynamical Models of the Terrestrial Climate, Adv. Geophys., 20(C), 183–304, doi:10.1016/S0065-2687(08)60324-6, 1978.

List of changes in the main manuscript "The dynamical core of the Aeolus 1.0 Statistical-Dynamical Atmosphere Model: Validation and Parameter Optimization"

p. 1, l. 1: changed title from "**The Dynamical Core of the Aeolus 1.0 Statistical-Dynamical Atmosphere Model: Validation and Parameter Optimization**" to "**The dynamical core of the Aeolus 1.0 Statistical-Dynamical Atmosphere Model: Validation and Parameter Optimization**"

p. 1, l. 14 – 20 changed to

"**We present and validate a set of equations for representing the atmosphere's large-scale general circulation in an Earth System Model of Intermediate Complexity (EMIC). These dynamical equations have been implemented in Aeolus 1.0, which is a Statistical-Dynamical Atmosphere Model (SDAM) and includes radiative transfer and cloud modules (Coumou et al., 2011; Eliseev et al., 2013). The statistical dynamical approach is computationally efficient, and thus enables us to perform climate simulations at multi-millennia timescales, which is a prime aim of our model development. Further, this computational efficiency enables us to scan large and high-dimensional parameter space to tune the model parameters for e.g. sensitivity studies.**

Here, we present novel equations for the large-scale zonal mean wind as well as those for planetary waves. Together with synoptic parameterization (as presented by Coumou et al., 2011), these form the mathematical description of the dynamical core of Aeolus 1.0.

We optimize the dynamical core parameter values by tuning all relevant dynamical fields to ERA-Interim reanalysis data (1983-2009) forcing the dynamical core with prescribed surface temperature, surface humidity and cumulus cloud fraction. We test the model's performance in reproducing the seasonal cycle and the influence of ENSO. We use a Simulated Annealing optimization algorithm, which approximates the global minimum of a high-dimensional function."

p. 1, l. 21 – 24 changed to

"**We optimize the dynamical core parameter values by tuning all relevant dynamical fields to ERA-Interim reanalysis data (1983-2009) forcing the dynamical core with prescribed surface temperature, surface humidity and cumulus cloud fraction. We test the model's performance in reproducing the seasonal cycle and the influence of ENSO. We use a Simulated Annealing optimization algorithm, which approximates the global minimum of a high-dimensional function.**"

p. 1, l. 32 added "**improvements and**"

p. 2, l. 2 changed "**Earth system model of intermediate complexity**" to "**Earth System Model of Intermediate Complexity**"

p. 2, l. 7 changed "**General circulation models**" to "**General Circulation Models**"

p. 2, l. 12 changed "**one- or two dimensional**" to "**1- or 2 dimensional**"

p. 2, l. 15 changed "**intermediate complexity climate models (EMICs)**" to "**Earth System Models of Intermediate Complexity (EMICs)**"

p. 2, l. 16 changed "**very**" to "**highly**"

p. 2, l. 19 changed "**(Eliseev et al., 2014a, 2014b; Ganopolski et al., 2001; Montoya et al., 2005)**" to "**(Eliseev et al., 2014a, 2014b; Ganopolski et al., 2001; Montoya et al., 2005)**"

p. 2, l. 22 removed "**different**"

p. 2, l. 25 added "**being**"

p. 2, l. 28 added "**the**"

p. 2, l. 29 removed comma

p. 2, l. 30 added paragraph

"**EMICs have been used in many climate studies and several different types of simplified atmospheric components that form part of an EMIC exist including 2-dimensional, zonally averaged atmosphere models, 2.5-dimensional atmosphere models (the vertical dimension is reconstructed using 2-dimensional fields) with a simple energy balance, or Statistical-Dynamical Atmosphere Models (SDAMs) (Claussen et al., 2002; McGuffie and Henderson-Sellers, 2005). Most EMIC studies focus on climate variability on very long timescales (e.g. glacial cycles), and therefore fast processes are normally parameterized. In particular, SDAMs parameterize smaller scale (and more short-lived) processes like synoptic eddy activity in terms of the large-scale, long-term fields. The assumption of those models is thus that atmospheric variables can be expressed in separate terms of a large-scale, long-term component, with characteristic spatial and temporal scales of L>1000 km and T>10 days, and a small-scale component like ensembles of synoptic-scale eddies and waves. The latter are then parameterized by their averaged statistical characteristics (e.g. their total kinetic energy and heat, their moist and momentum fluxes, …). This means that transport effects of the fast moving weather systems on the large-scale, long-term atmospheric motion are averaged (Ehlers et al., 2001).**

The essential difference to GCMs is the point of truncation in the frequency spectrum of atmospheric motion (Saltzman, 1978). GCMs solve all phenomena of frequencies lower than and including synoptic cyclones (and sometimes even mesoscale systems), whereas Statistical-Dynamical (SD) models parameterize all scales smaller and equal to synoptic. Much of the difficulty in SD models is to define physically reasonable parameterizations occurring in the equations (Saltzman, 1978). For Aeolus the synoptic parameterization has been described in detail in Coumou et al. (2011).

As written above, SD models are also spatially averaged since for long-term climate simulations, we are typically interested in the large spatial aspects of the climate. It is further practical to split the large-scale, long-term field into two components: the zonally averaged mean field, and the asymmetric departure of the field from the zonally averaged fields characterizing the East-West variations. The azonal variables can be, for example, resolved by 1-dimensional Fourier components around latitude circles or into spherical harmonics (Saltzman, 1978).

Here, we present the Aeolus 1.0 dynamical core, developed at the Potsdam Institute for Climate Impact Research (PIK), a new SD model for the atmosphere. It uses some aspects of the atmosphere module of the EMIC CLIMBER-2 developed by Petoukhov et al. (2000). The dynamical core is completely new with novel equations for the large-scale meridional wind speed as well as quasi-stationary planetary waves. Together with the synoptic parameterizations presented in Coumou et al. (2011), these equations form the new dynamical core of Aeolus 1.0. The model is coupled with the cloud module consisting of a 3-layer stratiform plus convective cloud scheme as presented and validated in Eliseev et al. (2013).

Further, we present the equations of the model and validate the dynamical core using a parameter optimization experiment. Aeolus 1.0 is forced with prescribed surface temperature, surface humidity and cumulus cloud fraction to test the model's performance. In particular we examine the reproduction of the seasonal cycle and the influence of ENSO and compare relevant dynamical fields of the model output against seasonal means of ERA-Interim reanalysis data (climatology 1983-2009). The effects of parameter tuning are evaluated to improve the performance of the model."

p. 2, l. 31 added "**novel**"

p. 2, l. 31 added "**1.0**"

p. 2, l. 32 changed "**Suppl. Mat.**" To "**Supplementary Information (S1 – S2)**"

p. 2, l. 33 added "**(which includes low-level, mid-level and upper-level stratiform clouds)**"

p. 3, l. 1 changed "**Coupled Climate Modeling Experiment** " to "**Coupled Model Intercomparison Project**"

p. 3, l. 7 – 10 changed to

"**Aeolus 1.0 is a 2.5-dimensional SD model, with the vertical dimension being largely parameterized and only coarsely resolved and it therefore belongs to the class of intermediate complexity atmosphere models. Water and energy conservations is achieved via a set of 2-dimensional, vertically averaged prognostic equations for temperature and specific humidity (Petoukhov et al., 2000).**"

p. 3, l. 11 added "**surface**"

p. 3, l. 11 added paragraph

"**For given temperature and specific humidity fields, the 3-dimensional wind field is calculated using a set of diagnostic equations. These statistical-dynamic equations for the wind fields are coupled and thus need several time steps or iterations to equilibrate.**"

p. 3, l. 13 – 26 changed to

"**The equations of the dynamical core of Aeolus 1.0 are separated into equations for the (1) synoptic-scale transient waves (or storm tracks), (2) quasi-stationary planetary waves and (3) the zonal-mean wind. Thus, following classical statistical-dynamical approaches (Dobrovolski, 2000; Imkeller and von Storch, 2012), the key assumption is that the wind velocity field V can be split into a synoptic scale component V' (2-6 days period) and a large-scale long-term component $\langle V \rangle$ (Fraedrich and Böttger, 1978) such that**

$$V = \langle V \rangle + V' = \{\langle u \rangle, \langle v \rangle, \langle w \rangle\} + \{u', v', w'\} \quad (1)$$

The large-scale, zonal-mean zonal wind velocity $\overline{\langle u(z, \phi) \rangle}$ with height above surface *z* and latitude ϕ is assumed to be geostrophic (resulting in the thermal wind balance):

$$\overline{\langle u(z,\phi) \rangle} = -\frac{1}{a\,f}\left(\frac{1}{\rho_0}\langle\overline{\frac{\partial p_0}{\partial \phi}}\rangle + \int_0^z \frac{g}{T_0}\langle\overline{\frac{\partial T}{\partial \phi}}\rangle \,\mathrm{d}z\right), \quad (2)$$

where the sea level pressure gradient is calculated by $\langle\overline{\frac{\partial p_0}{\partial \phi}}\rangle = \frac{a v^* \rho |f|}{-C_\alpha \sin\alpha}$ with ageostrophic velocity parameter $C_\alpha = 5$ and the Earth radius a (derived and explained by Pethoukov et al. (2000), eq.(13)) and α is the cross-isobar angle defined as in Coumou et al. (2011), eq. (A31). The variable v^* is the azonal meridional wind velocity,

ρ is the air density with the reference air density ρ_0, f the Coriolis parameter, ϕ is the latitude, T_0 is the reference temperature and g the gravitational acceleration (see Petoukhov et al., 2000).

"

p. 3, l. 27 changed "**S1.2**" to "**the Suppl. Inf. in S2**"

p. 3, l. 27 changed "**large scale**" to "**large-scale**"

p. 4, l. 1 changed to

"

$$\overline{\langle v(z,\phi)\rangle} = \frac{d1 * (-2\tan(\phi)\left(\overline{\langle u^* v^*\rangle} + \overline{\langle u' v'\rangle}\right)) + d2 * (\frac{\partial}{\partial\phi}\left(\overline{\langle u^* v^*\rangle} + \overline{\langle u' v'\rangle}\right)) + d3 * ((-\frac{dK_z}{dz} + \frac{K_z}{H_0})\frac{\partial\overline{\langle u\rangle}}{\partial z}a) + d4 * (A)}{n1 * (\tan(\phi)\overline{\langle u\rangle}) + n2 * \left(-\frac{\partial\overline{\langle u\rangle}}{\partial\phi}\right) + n3 * (2\Omega a\sin(\phi))}, \quad (3)$$

Where d_1, d_2, d_3, d_4, n_1, n_2 and n_3 are tunable parameters and A represents the convection-related term

$$A = \frac{\mathcal{L}\overline{\langle P_{co}\rangle}}{H_0}\frac{\overline{\langle u_{sf}\rangle}}{\Gamma_a - \Gamma_0 - \Gamma_1(T_a - T_0)\left(1 - a_q q_s^2\right) + \Gamma_2 n_c}.$$

"

p. 4, l. 4-9 changed to

"**The atmospheric scale height H_0, the exchange for the momentums K_z, the the Earth's angular velocity Ω as well as the dry adiabatic lapse rate Γ_a, latent heat of evaporation $\mathcal{L}$ and model parameters Γ_0, Γ_1, Γ_2, a_q, T_0 are explained in Table 1. T_a is a temperature which would occur near the surface if the lapse rate did not change within the planetary boundary layer (PBL), q_s is the surface air specific humidity and n_c is the cumulus cloud amount. The latter variable is either computed by the cloud module or, as in this experiment, observational data is used. The variable P_{co} is the convective precipitation rate and is calculated by the cloud model (Eliseev et al., 2013). The variable u_{sf} is the zonal surface wind, see eq. (S10) in the Suppl. Information.**

"

p. 4, l. 10 added "**large-scale**"

p. 4, l. 10 removed "**the**"

p. 4, l. 13 added "**1/a**"

p. 4, l. 14 added "**1/a**"

p. 4, l. 18-19 changed to "v^*_{EBL} **itself. The equation for the orographically induced waves is introduced in the Suppl. Inf. S1.2.**"

p. 4, l. 21 changed "**Information**"to "**Inf. S1.3**"

p. 5, l. 1-4 changed to

"**The zeroth order solution of the thermally induced waves of the barotropic vorticity equation is given by (see Suppl. Inf. S1.3.):**

$$\langle \psi^*_{th,0,EBL} \rangle = -\langle T^*_{EBL} \rangle \frac{g}{\Omega \rho_0 T_0^2 \cos \phi} \nabla_\phi \int_0^{z_{EBL}} \rho \langle [T(z)] \rangle \, dz \qquad (8)$$

It is solved at two beta-planes, for the Northern and Southern Hemisphere, respectively:

$$\langle \psi^*_{th,0,EBL} \rangle_{NH} = -\langle T^*_{EBL} \rangle \frac{g}{\Omega \rho_0 \, T_0^2 \cos \beta_{NH}} \nabla_\phi \int_0^{z_{EBL}} \rho \langle [T(z)] \rangle \, dz \qquad (9)$$

$$\langle \psi^*_{th,0,EBL} \rangle_{SH} = -\langle T^*_{EBL} \rangle \frac{g}{\Omega \rho_0 \, T_0^2 \cos \beta_{SH}} \nabla_\phi \int_0^{z_{EBL}} \rho \langle [T(z)] \rangle \, dz \qquad (10)$$

The beta-plane is an approximation, in which the Coriolis parameter is linearized to a reference latitude, β_{NH} and β_{SH} for the Northern Hemisphere and Southern Hemisphere, respectively. In the tropical belt the variable $\langle \psi^*_{th,0,EBL} \rangle$ is interpolated linearly between the two beta-planes."

p. 5, l. 5 - 6 changed to "**The standardized integrated heat content in equation (8) ($I_v = \int_0^{z_{EBL}} \rho \langle [T(z)] \rangle \, dz$) is calculated analytically by assuming a lapse rate $\Gamma = \Gamma_0 + \Gamma_1 (T_a - T_0)\left(1 - a_q q_s^2\right) - \Gamma_2 n_c$ such that $T(z) = T(z_{EBL}) - \Gamma (z - z_{EBL})$.**"

p. 5, l. 8 changed "**5**" to "**five**"

p. 5, l. 11 change "**level**" to "**levels**"

p. 5, l. 12 change "**Mat.**" To "**Inf. S1.1**"

p. 5, l. 13 added "**Finally, the**"

p. 5, l. 14 removed colon.

p. 5, l. 15 added paragraph

"**Since detailed derivations are provided in Coumou et al. (2011), we only briefly discuss the diagnostic equations for transient eddy activity here. The equations are derived starting from the equation of the kinetic energy of transient eddies:**"

p. 5, . l. 16 – 21 changed to

"**Since detailed derivations are provided in Coumou et al. (2011), we only briefly discuss the diagnostic equations for transient eddy activity here. The equations are derived starting from the equation of the kinetic energy of transient eddies:**

$$\frac{\partial \langle E'_k \rangle}{\partial t} = -\langle V \rangle \cdot \nabla \langle E'_k \rangle + \langle u'V' \rangle \cdot \nabla \langle u \rangle - \langle v'V' \rangle \cdot \nabla \langle v \rangle + K_{fh} \Delta_H \langle E'_k \rangle + K_{fz} \Delta_z \langle E'_k \rangle - K_{fs} \langle E'_k \rangle + f\left(\langle u'v'_{ag} \rangle - \langle v'u'_{ag} \rangle\right) \qquad (11)$$

"

p. 5, l. 20 changed "**equiportioned**" to "**equipartioned**"

p. 5, l. 20 added "**the**"

p. 5, l. 21 changed "**the Eq. (9)**" to "**Eq. (11)**"

p. 5, l. 22 added paragraph

"**Here, K_{fh} and K_{fz} are internal atmospheric small-/meso-scale friction coefficients in the horizontal and vertical direction respectively, K_{fs} is the surface friction coefficient, f the Coriolis parameter and the subscript "*ag*" denotes ageostrophic terms.**

The terms for K_{syn}, the vertical macro-turbulent diffusion coefficient, and $f\left(\langle v'v'_{ag}\rangle - \langle u'u'_{ag}\rangle\right)$ need to be parameterized which is derived in Coumou et al. (2011). This way, a set of diagnostic equations for synoptic transient eddies is derived which, as also seen in equations (12) − (14), are all coupled to the large-scale wind field."

p. 6, l. 16 – 27 changed to

"T**he simulations were forced by multi-year averages of monthly mean climatological, El Niño and La Niña months data (surface temperature, surface specific humidity, temperature at 500mb, geopotential height at 500mb and 1000mb) using ERA-Interim Reanalysis Data (Dee et al., 2011) for 1983-2009 as our aim is that Aeolus captures year-to-year variability associated with the ENSO cycle. We identified 87 El Niño (74 La Niña) months using 3 month running means of ERSST v4 anomalies (Huang et al., 2016) using the definition that at least 5 consecutive overlapping seasons of SST anomalies are greater than 0.5K (less than -0.5K) for El Niño (La Niña) events.**

Multi-year averages of monthly mean, El Niño and La Niña months cumulative cloud fraction are taken from ISSCP (Rossow and Schiffer, 1999). The spatial resolution is 2.5×2.5 degrees $\mathrm{lat} \times \mathrm{lon}$ and the time range is 1983-2009. We chose this time period, because the cumulative cloud fraction data, which is needed to calculate the lapse rate is only available for this time period."

p. 6, l. 31 – p. 7, l. 7 removed spaces between numbers and units

p. 7, l. 2 added "**the**"

p. 7, l. 4 changed "**profile realistic**" to "**realistic profile**"

p. 7, l. 7 added "**parameters for the**"

p. 7, l. 8 changed "$p = 500$ **mb**" to "**500mb**"

p. 7, l. 8 changed "**Ferrel**" to "**Ferrell**"

p. 7, l. 10 removed spaces between numbers and units

p. 7, l. 18 removed "$\mathrm{lat} \times \mathrm{lon}$"

p. 7, l. 19 changed "**ca**." to "**approx**."

p. 7, l. 21 – 22 changed to "**The equations (1) – (14) are implemented in Aeolus and numerically solved on a 3.75×3.75 degrees reduced grid with 4 tropospheric height levels (1000m, 3000m, 5000m, 9000m).** "

p. 7, l. 29 – p. 8, l. 2 changed to

"**A common approach for parameter tuning is Simulated Annealing (Ingber, 1996; Kirkpatrick, 1984). It is one experiment type in the multi-run simulation environment SimEnv for sensitivity and uncertainty analysis of model output (Flechsig et al., 2013) which we use for all calibration experiments. A schematic plot of the optimization process is shown in Suppl. Inf. S3.**

For each model run, the thermal state of the atmosphere is kept constant (and initialized as described above) and the dynamical core is equilibrated to this thermal state. This typically requires only a few time steps. Since we tune only the parameters of the dynamical core, Aeolus first calculates the clouds using its cloud scheme (Eliseev et al., 2013) to determine the lapse rate and initialize the 3-dimensional thermal state. After that only the state of the dynamical core is updated each time step"

p. 8, l. 3 changed "**Core**" to "**core**"

p. 8, l. 4 changed "**optimised**" to "**optimized**"

p. 8, l. 6 – 8 changed to

"**For the azonal wind velocities we use a weighting function which excludes the tropics (from 10°S to 10°N) and polar regions (poleward of 60°S for the Southern Hemisphere to exclude influences of Antarctica and poleward of 70°N for the Northern Hemisphere) such that the mid-latitudes, where planetary waves are important, are optimized.**"

p. 8, l. 19 changed "**Core**" to "**core**"

p. 9, l. 2 – 3, removed "**The skill score function for the mass flux consists of the product of the correlation of observation and model as well as the mean mass flux of the Hadley cell.**"

p. 9, l. 6 changed "**fields**" to "**mean mass flux**"

p. 9, l. 19 changed "**6**" to "**six**"

p. 9, l. 22-23 changed to "**In Figure 1 and Figure 2 the azonal component of the zonal wind velocities ($\langle u^* \rangle$) for February and August at 500mb are displayed, respectively.**"

p. 10, l. 1 – 9 changed to

"**In Figure 5 the zonal-mean zonal wind velocity ($\langle u \rangle$) at 500mb is shown with the orange line representing reanalysis data, red representing model data with optimized parameters, and gray representing model data with pre-optimized parameters. The figure is subdivided into six subplots: The top row depicts $\langle u \rangle$ in February and the bottom row shows $\langle u \rangle$ in August, while the columns show climatological data, El Niño data and La Niña data, respectively. It is noticeable that the results obtained with pre-optimized parameters are already reasonable. Apparently the initial choice of tuning parameter values were already near the optimum and hence the optimized parameters lead only too small improvements of the model results. The Northern Hemisphere $\langle u \rangle$ profile is well resolved in both seasons for both El Niño and La Niña months. Parameter optimization slightly improves the results in the tropics. The modeled amplitude of $\langle u \rangle$ in the Southern Hemisphere is too small in February for all plots, and too high in August.**"

p. 10, l. 11 added "**than the pre-optimized parameter values**"

p. 10, l. 12 changed "**velocities**" to "**speeds**"

p. 10, l. 18 – 23 changed to

"**Here, the gain of the parameter optimization is clearly better than we saw with calibration step 1. The ENSO cycle is clearly visible. However, the width of the Hadley cell (especially in August) is still too small compared to the width of the Hadley cell obtained by reanalysis data. The figure shows only plots with a latitudinal range from 60°S to 90°N as reanalysis data is spikey over Antarctica.**"

p. 10, l. 27 changed to "**The parameter optimization gained more improvement in NH than in SH.**"

p. 10, l. 29 changed "**energy $\overline{\langle E'_K \rangle}$.**" to "**energies $\langle E'_K \rangle$** "

p. 10, l. 29 changed "**is**" to "**are**"

p. 10, l. 32 changed "$\overline{\langle E'_K \rangle}$." To "$\langle E'_K \rangle$"

p. 10, l. 32 shifted "for both climatology and El Niño" to the end of the sentence

p. 11, l. 1 changed "$\overline{\langle E'_K \rangle}$." To "$\langle E'_K \rangle$"

p. 11, l. 3 changed "$U0$" to "U_0"

p. 11, l. 5 – 7 changed to "**The parameters d_3 and n_3 are close to 1, whereas the parameters d_2, d_4 and n_1 are close to 2 and have a strong impact on the amplitude of the Hadley cell and the Ferrell cell. The parameter with the smallest influence is d_1.**"

p. 11, l. 9 changed "**$\overline{\langle m \rangle}$"** to "**$\overline{\langle m \rangle}$"**

p. 11, l. 9 added "**models"**

p. 11, l .13 removed "**as"**

p. 11, l. 14 changed "**$\overline{\langle m \rangle}$"** to "**$\overline{\langle m \rangle}$"**

p. 11, l. 15 changed "**$\overline{\langle m \rangle}$"** to "**$\overline{\langle m \rangle}$"**

p. 11, 17 changed "**Aeolus**" to "**Aeolus'** "

p. 11, l. 21 – 25 changed to "**In this paper we presented the atmosphere model Aeolus, which is a Statistical-Dynamical Atmosphere Model and belongs to the class of intermediate complexity models. The equations of Aeolus are time-averaged and the model has a spatial resolution of $3.75° \times 3.75°$ degrees lat $\times$ lon. The 3-dimensional structure of Aeolus is reconstructed using a set of 2-dimensional, vertically averaged prognostic equations for temperature and water vapor (Petoukhov et al., 2000).**"

p. 11, l. 28 removed "**which is in a high parameter range**"

p. 11, l. 28 removed Italic font

p. 11, l. 30 changed "**At first**" to "**First**"

p. 11, l. 32 changed "**atmospheres**" to "**atmosphere"**

p. 12, l. 1 changed "**season**" to "**seasonal**"

p. 12, l. 5 changed "**Antarctica**" to "**Antarctic**"

p. 12, l. 6 removed "**coupled**"

p. 12, l. 22 added "**Data**"

p. 13, l. 14 changed to "**Dobrovolski, S. G.: Stochastic Climate Theory, Springer-Verlag Berlin Heidelberg, 2000.**"

p. 13, l. 14 added "**Ehlers, E. and Krafft, T.: Understanding the Earth System: Compartments, Processes and Interactions, Springer-Verlag, Berlin, Heidelberg, 2001**."

p. 13, l. 24 - 26 changed to "**Flechsig, M., Böhm, U., Nocke, T. and Rachimow, C.: The Multi-Run Simulation Environment SimEnv, , 1,. [online] Available from: https://www.pik-potsdam.de/research/transdisciplinary-concepts-and-methods/tools/simenv/, 2013.**"

p. 13, l. 27 – 29 changed to "**Ganopolski, aA., Petoukhov, V., Rahmstorf, S., Brovkin, V., Claussen, M., Eliseev, aA. V. and Kubatzki, C.: Climber-2: A climate system model of intermediate complexity. Part II: Model sensitivity, Clim. Dyn., 17, 735–751, doi:10.1007/s003820000144, 2001.**"

p. 14, l. 5, removed "**doi:10.1.1.15.2777**"

p. 14, l. 8 added "**Kirkpatrick, S.: Optimization by simulated annealing: Quantitative studies, J. Stat. Phys., 34, 975–986, doi:10.1007/BF01009452, 1984.**"

p. 14, l. 12 added "**McGuffie, K. and Henderson-Sellers, A.: A Climate Modelling Primer, 3rd ed., J. Wiley and Sons, 2005.**"

p. 14, l. 21 added "**Rossow, W. B. and Schiffer, R. A.: Advances in Understandig Clouds from ISCCP, Bull. Amer. Meteor. Soc., 80(11), 2261–2287, doi:10.1175/1520-0477(1999)080<2261:AIUCFI>2.0.CO;2, 1999.**

Saltzman, B.: A Survey of Statistical-Dynamical Models of the Terrestrial Climate, Adv. Geophys., 20(C), 183–304, doi:10.1016/S0065-2687(08)60324-6, 1978."

p. 14, l. 23 added "**Taylor, K. E.: Summarizing multiple aspects of model performance in a Single Diagram, J. Geophys. Res., 106(D7), 7183–7192, doi:10.1029/2000JD900719, 2001.**"

p. 15, l. 1 -3 changed to "**Figure 1 Azonal large-scale zonal wind u* at 500mb for all February months/ El Niño February months/ La Niña February months. The left column shows the results from reanalysis data and the right column shows the results from Aeolus received by optimized parameters. The model is forced by surface temperature, humidity and cumulus cloud fraction.**"

p. 16, l. 1 changed to "**Figure 2 Azonal large-scale zonal wind velocity u* at 500mb for August (compare Fig. 1).**"

p. 17, l. 1 changed to "**Figure 3 Azonal large-scale meridional wind velocity v* at 500mb for February (compare Fig. 1).**"

p. 17, l. 2 changed to "**Figure 1 Azonal large-scale meridional wind velocity v* at 500mb for August (compare Fig. 1).**"

p. 18, l. 1 - 10 changed to "**Figure 2 Zonal-mean large-scale zonal wind velocity $\overline{\langle u(z,\phi)\rangle}$ at 500mb. (a) shows the climatological monthly mean zonal-mean zonal velocity in February, (b) depicts the monthly mean zonal-mean velocity of El Niño Februaries and (c) the monthly mean zonal-mean velocity of La Niña Februaries. (d) displays the monthly mean climatological zonal-mean zonal velocity in August, (e) shows the monthly mean zonal-mean velocity in El Niño Augusts and (f) depicts the monthly mean zonal-mean velocity in La Niña Augusts. The yellow**

line represents zonal-mean large-scale zonal wind obtained by reanalysis data, the gray line is zonal-mean large-scale zonal wind velocity from Aeolus using pre-optimized parameters, and the red line represents zonal-mean large-scale zonal wind velocity from Aeolus using optimized parameters."

p. 19, l. 1 - 8 changed to "**Figure 6 Zonal-mean large-scale mass flux (⟨m⟩)‾. (a) shows the climatological monthly mean zonal-mean mass flux in February, (b) depicts the monthly mean zonal-mean mass flux of El Niño Februaries and (c) the monthly mean zonal-mean mass flux of La Niña Februaries. (d) displays the monthly mean climatological zonal-mean mass flux in August, (e) shows the monthly mean zonal-mean mass flux in El Niño Augusts and (f) depicts the monthly mean zonal-mean mass flux in La Niña Augusts. The yellow line represents zonal-mean large scale mass flux obtained by reanalysis data, the gray line is the zonal-mean large scale mass flux from Aeolus using pre-optimized parameters, and the red line represents the zonal-mean large scale mass flux from Aeolus using optimized parameters.**"

p. 20, l. 1 changed to "**Figure 3 Zonal-mean time averaged eddy kinetic energy $\overline{\langle E'_k \rangle}$ (compare Fig. 6).**"

p. 21, l. 1 changed to "**Figure 4 Eddy kinetic energy $\langle E'_k \rangle$ in February at 500mb (compare Fig. 1).**"

p. 22, l. 1 changed to "**Figure 5 Eddy kinetic energy $\langle E'_k \rangle$ in August at 500mb (compare Fig. 1).**"

p. 23, l. 1 changed to "**Figure 6 Comparison to CMIP5-Models. The orange line represents Era Interim data, the red line results from Aeolus and grey lines CMIP5 Models (annuak mean zonal-mean data).**"

p. 24, l. 8 changed "**parameters**" to "**parameter**"

p. 24, l. 10 changed "**parameters**" to "**parameter**"

p. 24, l. 11 changed "**parameters**" to "**parameter**"

List of changes in the Supplementary Information "The dynamical core of the Aeolus 1.0 Statistical-Dynamical Atmosphere Model: Validation and Parameter Optimization"

p. 1, l. 1: changed title from "S1 **Supplementary Material**" to "**Supplementary Information**"

p. 1, l. 3 changed "**S1.1 Planetary Waves**" to "**S1 Planetary Waves**"

p. 1, l. 4- 9, changed to "

S1.1 Calculation of planetary waves at tropospheric levels excluding EBL-level

At other tropospheric levels than the EBL, the components are calculated by

$$\langle u^*(z)\rangle = -\frac{1}{f\rho_0}\nabla_\phi\langle p_z^*\rangle \qquad \textbf{(S1)}$$

$$\langle v^*(z)\rangle = \frac{1}{f\rho_0}\nabla_\lambda\langle p_z^*\rangle, \qquad \textbf{(S2)}$$

The azonal component is computed assuming isothermal expansion of air parcels in planetary waves"

p. 1, l. 14 – p. 2, . 8 changed to "**S1.2 Orographically induced stream function**

For the waves excited by the orography, the stream function is calculated by

$$\beta\nabla_\lambda\langle\psi^*_{or,0,EBL}\rangle = -\frac{f}{H_0}\langle w_{or}\rangle + \frac{f^2}{g}\frac{\partial\langle u'v'\rangle^*}{\partial z} \qquad \textbf{(S5)}$$

where f is the Coriolis parameter and $\beta = \nabla_\phi f$ and

$$w_{or} = \langle u\rangle\nabla_\phi h_{or} + \langle v\rangle\nabla_\lambda h_{or} + a_{std}(\langle u\rangle^2 + \langle v\rangle^2 + \langle u'^2\rangle + \langle v'^2\rangle)^{1/2}h_{std}. \qquad \textbf{(S6)}$$

The variable h_{or} describes the grid cell averaged orography height h_{std} the subgrid scale standard deviation of the height of mountains, and $a_{std}$is an additional tuning parameter.

The azonal component describes quasi-stationary planetary waves and is subdivided into a geostrophic and ageostrophic term:

$$\boldsymbol{u^* = u^*_{geos} + u^*_{ageos}}$$

$$\boldsymbol{v^* = v^*_{geos} + v^*_{ageos}}$$

"

p. 2, l. 9 added paragraph "**S1.3 Zeroth order solution of the thermally induced waves of the barotropic vorticity equation at the EBL**

We start from the z-projection of the baroclinic vorticity equation, which can be derived from the simplified Navier-Stokes-equation :

$$\boldsymbol{\overline{u}\frac{\partial}{\partial x}\left(\frac{\partial^2\langle\Psi^*_{EBL}\rangle}{\partial x^2}+\frac{\partial^2\langle\Psi^*_{EBL}\rangle}{\partial y^2}\right)+\beta\frac{\partial\langle\psi^*\rangle}{\partial x}=-\frac{\rho}{T_0}\frac{\partial\langle T^*_{EBL}\rangle}{\partial x}\frac{\partial\overline{\mathrm{p}}}{\partial y}\frac{1}{{\rho_0}^2}} \quad \textbf{(S7)}$$

with $\boldsymbol{\beta=\frac{2\Omega}{a}\cos\phi}$, and $\boldsymbol{\Omega}$ is the earth's rotation angular velocity, $\boldsymbol{a}$ is the earth's radius and $\boldsymbol{\phi}$ the latitude.

In Eq. (S7) $\boldsymbol{\langle\Psi^*_{EBL}\rangle}$ is the stream function of the azonal large-scale component at the equivalent barotropic level $\boldsymbol{z_{EBL}}$, $\boldsymbol{x}$ and $\boldsymbol{y}$ are the horizontal and vertical direction, $\boldsymbol{T_0}$ is the constant reference temperature and $\boldsymbol{\langle T^*_{EBL}\rangle}$ is the large-scale long-term azonal temperature at the EBL. The variable $\boldsymbol{\overline{u}}$ is the zonal mean zonal wind velocity, $\boldsymbol{\rho_0}$ stands for the density near surface and $\boldsymbol{\overline{\mathrm{p}}}$ is the zonal mean pressure.

For the stream function of the azonal large-scale component of motion at the equivalent barotropic level $\boldsymbol{z_{EBL}}$we use the ansatz

$$\boldsymbol{\langle\Psi^*_{EBL}\rangle=\langle\Psi^*_{0,EBL}\rangle+\epsilon\langle\Psi^*_{1,EBL}\rangle+\ldots}$$

For the zeroth order approximation, we can neglect higher order derivations of $\boldsymbol{\Psi}$:

$$\boldsymbol{\beta\frac{\partial\langle\Psi^*_{0,EBL}\rangle}{\partial x}=-\frac{1}{\rho\,T_0}\frac{\partial\langle T^*_{EBL}\rangle}{\partial x}\frac{\partial}{\partial y}\frac{\int_0^\infty\rho\langle[T(z)]\rangle\,dz}{H_0}} \quad \textbf{(S8)}$$

In eq. (S8), we replaced $\boldsymbol{\overline{\mathrm{p}}=\int_0^\infty R\rho\langle[T(z)]\rangle\,dz/H_0}$ and $\boldsymbol{H_0=RT_0/g}$ and $\boldsymbol{\rho=\rho_0\exp(-z/H_0)}$, $\boldsymbol{R}$ is the gas constant, $\boldsymbol{\rho}$ is the air density, T is the temperature , $\boldsymbol{H_0}$ is the atmospheric scale height, and $\boldsymbol{g}$ the gravity acceleration . Per definition, one can replace the term with

$$\boldsymbol{\frac{\int_0^\infty p\,dz}{H_0}=\frac{gR}{RT_0}2\int_0^{z_{EBL}}\rho\langle[T(z)]\rangle\,dz}$$

Such that

$$\frac{\partial\langle\psi^*_{0,EBL}\rangle}{\partial x} = -\frac{agR}{2\Omega RT_0^2\rho_0\cos\phi}2\frac{\partial}{\partial y}\int_0^{z_{EBL}}\rho\langle[T(z)]\rangle\,dz\frac{\partial\langle T^*_{EBL}\rangle}{\partial x}$$

With latter equation and $\frac{1}{a}\nabla_\phi = \partial/\partial y$ **, we can then derive**

$$\langle\psi^*_{0,EBL}\rangle = -\langle T^*_{EBL}\rangle\frac{g}{\Omega\rho_0 T_0^2\cos\phi}\nabla_\phi\int_0^{z_{EBL}}\rho\langle[T(z)]\rangle\,dz$$

"

p. 2, l. 9, changed "**S1.2**" to "**S2**"

p. 2, l. 9 – p. 5, l. 2 reordered equation numbers

p. 2, l. 13 - 17, changed to "**With** $K_z = 0.005\,z$ **and**

$$A = \frac{\mathcal{L}\overline{\langle P_{co}\rangle}}{H_0}\frac{\overline{\langle u_{sf}\rangle}}{\Gamma_a - \Gamma_0 - \Gamma_1(T_a - T_0)(1 - a_q q_s^2) + \Gamma_2 n_c}$$

whereby the parameters are given in Table 1. We roughly approximate $\overline{\langle u_{sf}\rangle}$ **by constant profile for this experiment**

$$\overline{\langle u_{sf}\rangle} = \begin{cases} 2, & |\phi| > 40 \\ -2\cos\left(\phi\frac{\pi}{40^\circ}\right), & \text{otherwise} \end{cases} \quad \textbf{(S10)}$$

"

p. 2, l. 19 added paragraph "**The additional calculation of** $\overline{\langle u_{sf}\rangle}$ **instead of the calculated surface zonal velocity is done to avoid instabilities. Instabilities can emerge due to the strong positive feedback between the meridional temperature and vertical wind velocity, which lead to high latent heat. In nature these would be damped out but due to fixed troposphere height, we parameterize it in the above described way.**"

p. 3, l. 2 changed "V "to **"V"**

p. 3, l. 13-14 changed to

"**Due to a "gap" in the three-dimensional (period-wavelength-phase velocity) spectrum of atmospheric processes (see, e.g., Fraedrich & Böttger 1978, Coumou et al. 2011), the synoptic-scale component in its interaction with the large-scale long-term component of the atmospheric fields on the time scales about 10-20 days and longer could be, to a first approximation, represented (described) in terms of its ensemble (statistical) characteristics**

(the second and higher-order moments), and not as the individual eddies (Saltzman, 1978). We can simplify the terms $\langle \overline{u}v' \rangle = \langle u'\overline{v} \rangle = 0$. In addition, it is $\overline{\overline{u}\overline{v}} = \overline{u}\overline{v}$ due to quasi stationarity of both terms. It is also $\langle \frac{dx}{dt} \rangle = 0$ and $\langle \overline{u}\overline{v} \rangle = \langle \overline{u} \rangle \langle \overline{v} \rangle$ since the oscillations of $\overline{u}$ and $\overline{v}$ are very small and independent of each other."

p. 4, l. 6-7 changed to **"Also, the scale analysis attests that $\langle \overline{w} \rangle \frac{\partial \langle u \rangle}{\partial z}$ are small (Petoukhov et al., 2003)"**

p. 4, l. 16 changed "$\widetilde{\kappa}$ "to "K_z"

p. 5, l. 1 changed "$\frac{dK_z}{z}$ "to "$\frac{dK_z}{dz}$"

p. 5, l. 2 added "

The derived equation for the meridional velocity does not account for latent heat release associated with convective precipitation. To capture this additional term we include convective precipitation and finally introduce tuning parameters, which have values close to 1.

S3 Schematic plot of the optimization process

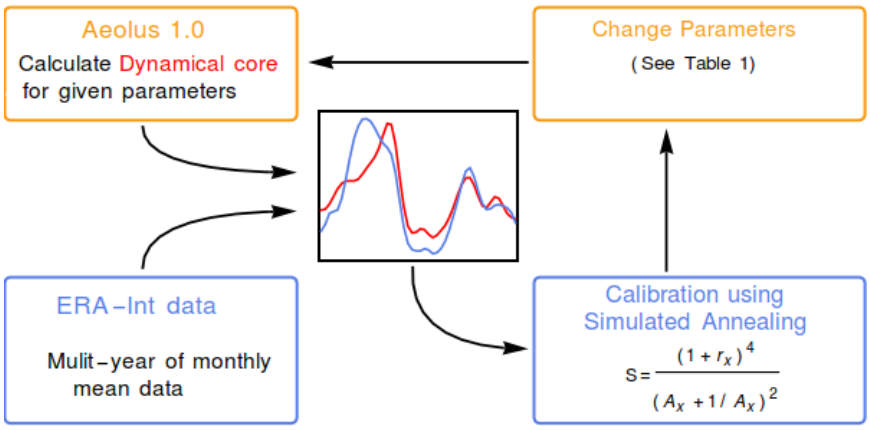

References

Hantel, M. and Hacker, J. M.: On the vertical eddy transports in the northern atmosphere. 1. Vertical eddy heat transport for summer and winter, J. Geophsical Res., 83, 1303–1318, 1978.

Petoukhov, V., Ganopolski, A. and Claussen, M.: POTSDAM - a set of atmosphere statistical-dynamical models: theoretical background, [online] Available from: https://www.pik-potsdam.de/research/publications/pikreports/.files/pr81.pdf, 2003.

Petoukhov, V., Rahmstorf, S., Petri, S. and Schellnhuber, H. J.: Quasiresonant amplification of planetary waves and recent Northern Hemisphere weather extremes, Proc. Natl. Acad. Sci. U. S. A.,

110(14), 5336–5341, doi:10.1073/pnas.1222000110, 2013.

Saltzman, B.: A Survey of Statistical-Dynamical Models of the Terrestrial Climate, Adv. Geophys., 20(C), 183–304, doi:10.1016/S0065-2687(08)60324-6, 1978.

Williams, G. P. and Davies, D. R.: A mean motion model of the general circulation, Q. J. R. Meteorol. Soc., (January), 471–489, 1965.

„

The ~~Dynamical Core~~dynamical core of the Aeolus 1.0 Statistical-Dynamical Atmosphere Model: Validation and Parameter Optimization

Sonja ~~Molnos~~[1]Totz[1,2], Alexey V. Eliseev[1,3,4,5], Stefan Petri[1], Michael Flechsig[1], Levke Caesar[1,2], Vladimir Petoukhov[1] and Dim Coumou[1,6]

[1] Potsdam Institute for Climate Impact Research, Potsdam, Germany
[2] Department of Physics, Potsdam University, Potsdam, Germany
[3]A.M. Obukhov Institute of Atmospheric Physics RAS, Moscow, Russia
[4] Kazan Federal University, Kazan, Russia
[5]Institute of Applied Physics, Russian Academy of Sciences, Nizhny Novgorod, Russia
[6]Institute for Environmental Studies (IVM), VU University Amsterdam
Correspondence to: S. ~~Molnos~~Totz (~~molnos~~sonja.totz@pik-potsdam.de)

Field Code Changed

~~**Abstract.** We present and validate a set of equations for representing the atmosphere's large-scale general circulation in an Earth system model of intermediate complexity (EMIC). These dynamical equations have been implemented in *Aeolus*, which is a Statistical Dynamical Atmosphere Model (SDAM) and includes radiative transfer and cloud modules (Coumou, 2011; Eliseev, 2013). The statistical dynamical approach is computationally efficient, and thus enables us to do climate simulations at multi millennia timescales, which is a prime aim of our model development. Further, this computational efficiency enables us to scan large and high-dimensional parameter space to tune the model parameters.~~

Abstract. We present and validate a set of equations for representing the atmosphere's large-scale general circulation in an Earth System Model of Intermediate Complexity (EMIC). These dynamical equations have been implemented in Aeolus 1.0, which is a Statistical-Dynamical Atmosphere Model (SDAM) and includes radiative transfer and cloud modules (Coumou et al., 2011; Eliseev et al., 2013). The statistical dynamical approach is computationally efficient, and thus enables us to perform climate simulations at multi-millennia timescales, which is a prime aim of our model development. Further, this computational efficiency enables us to scan large and high-dimensional parameter space to tune the model parameters for e.g. sensitivity studies.
Here, we present novel equations for the large-scale zonal mean wind as well as those for planetary waves. Together with synoptic parameterization (as presented by Coumou et al., 2011), these form the mathematical description of the dynamical core of Aeolus 1.0.

We optimize the dynamical core parameter values by tuning all relevant dynamical ~~variables~~fields to ERA-Interim reanalysis data (1983-2009) ~~using monthly mean data of climatology data as well as the data for the El~~

~~Niño and La Niña composites~~forcing the dynamical core with prescribed surface temperature, surface humidity and cumulus cloud fraction. We test the model's performance in reproducing the seasonal cycle and the influence of ENSO. We use a Simulated Annealing optimization algorithm, which approximates the global minimum of a high-dimensional function.

With non-tuned parameter values, the model performs reasonably in terms of its representation of zonal-mean circulation, planetary waves and storm tracks. The Simulated Annealing optimization improves in particular the model's representation of the northern hemisphere jet stream and storm tracks as well as the Hadley circulation.

The regions of high azonal wind velocities (planetary waves) are accurately captured for all validation experiments. The zonal-mean zonal wind and the integrated lower troposphere mass flux show good results in particular in the Northern Hemisphere. In the Southern Hemisphere, the model tends to produce too weak zonal-mean zonal winds and a too narrow Hadley circulation. We discuss possible reasons for these model biases as well as planned future model improvements and applications.

Keywords:

Earth ~~system model~~System Model of ~~intermediate complexity~~Intermediate Complexity, Statistical-~~-~~Dynamical Atmosphere Model, Optimization, model parameter tuning

1 Introduction

Numerical models of the Earth system play a key role in our understanding of physical processes in Earth and Atmosphere and can be used to simulate past and future climate changes.

General ~~circulation models~~Circulation Models (GCMs) are physically the most realistic tools for studying and modelling climate variability and climate change in the Earth system. However, due to their relatively high-resolution, they are costly in terms of CPU runtime, limiting their applicability to study climate variability over long (~millennia) timescales.

On the other hand, highly idealized and computational efficient models for the climate system are able to simulate long time periods, but those are often box~~-, one-~~ or ~~two-~~1- or 2-dimensional models describing only a limited number of processes or feedbacks of the real world. Hence their application is limited, but they have been applied to study paleo climate (Berger et al., 1992; Harvey, 1989) and future global change (Xiao et al., 1997).

A third class of models are so-called ~~intermediate complexity climate models~~Earth System Models of Intermediate Complexity (EMICs) which form a compromise between the computationally expensive (but more realistic) GCMs and the ~~very~~highly simplified models (Claussen et al., 2002). The number of processes and feedbacks are comparable to GCMs, however due to a reduction in resolution and/or complexity of some model components, it is possible to study climate simulations up to multi-millennia timescales ~~(Eliseev et al., 2014a, 2014b; Ganopolski et al., 2001; Montoya et al., 2005)~~(Eliseev et al., 2014a, 2014b; Ganopolski et al., 2001;

Montoya et al., 2005). Other applications include determining quick assessments of climate change impacts or run thousands of parameter sensitivity experiments (Knutti et al., 2002; Schmittner and Stocker, 1999).

EMICs are thus particularly useful for understanding the ~~different~~ roles of different Earth components on very long timescales (multi-millennia and longer) and consequently form useful tools complementary to GCMs. Internal climate processes on such very long timescales are primarily driven by ocean and ice dynamics (Holland et al., 2001; Latif, 1998; Polyakov et al., 2003), with the atmosphere's role being likely limited to globally distributing any perturbations to the system. In GCMs, it is however often the atmosphere which takes most of the computational load due to the need to resolve synoptic weather systems, which requires a high-resolution discretization in space and time. For these reasons, a key step in the development of EMICs intended for studying ocean and ice dynamics on multi-millennial timescales~~,~~ is the derivation and validation of statistical-dynamical equations which accurately represent atmosphere dynamics (Coumou et al., 2011).

Field Code Changed

EMICs have been used in many climate studies and several different types of simplified atmospheric components that form part of an EMIC exist including 2-dimensional, zonally averaged atmosphere models, 2.5-dimensional atmosphere models (the vertical dimension is reconstructed using 2-dimensional fields) with a simple energy balance, or Statistical-Dynamical Atmosphere Models (SDAMs) (Claussen et al., 2002; McGuffie and Henderson-Sellers, 2005). Most EMIC studies focus on climate variability on very long timescales (e.g. glacial cycles), and therefore fast processes are normally parameterized. In particular, SDAMs parameterize smaller scale (and more short-lived) processes like synoptic eddy activity in terms of the large-scale, long-term fields. The assumption of those models is thus that atmospheric variables can be expressed in separate terms of a large-scale, long-term component, with characteristic spatial and temporal scales of L>1000 km and T>10 days, and a small-scale component like ensembles of synoptic-scale eddies and waves. The latter are then parameterized by their averaged statistical characteristics (e.g. their total kinetic energy and heat, their moist and momentum fluxes, …). This means that transport effects of the fast moving weather systems on the large-scale, long-term atmospheric motion are averaged (Ehlers et al., 2001).

The essential difference to GCMs is the point of truncation in the frequency spectrum of atmospheric motion (Saltzman, 1978). GCMs solve all phenomena of frequencies lower than and including synoptic cyclones (and sometimes even mesoscale systems), whereas Statistical-Dynamical (SD) models parameterize all scales smaller and equal to synoptic. Much of the difficulty in SD models is to define physically reasonable parameterizations occurring in the equations (Saltzman, 1978). For Aeolus the synoptic parameterization has been described in detail in Coumou et al. (2011).

Formatted: Font color: Black, English (U.K.)

Formatted: English (U.K.)

As written above, SD models are also spatially averaged since for long-term climate simulations, we are typically interested in the large spatial aspects of the climate. It is further practical to split the large-scale, long-term field into two components: the zonally averaged mean field, and the asymmetric departure of the field from the zonally averaged fields characterizing the East-West variations. The azonal variables can be, for example, resolved by 1-dimensional Fourier components around latitude circles or into spherical harmonics (Saltzman, 1978).

Here, we present the Aeolus 1.0 dynamical core, developed at the Potsdam Institute for Climate Impact Research (PIK), a new SD model for the atmosphere. It uses some aspects of the atmosphere module of the EMIC

CLIMBER-2 developed by Petoukhov et al. (2000). The dynamical core is completely new with novel equations for the large-scale meridional wind speed as well as quasi-stationary planetary waves. Together with the synoptic parameterizations presented in Coumou et al. (2011), these equations form the new dynamical core of Aeolus 1.0. The model is coupled with the cloud module consisting of a 3-layer stratiform plus convective cloud scheme as presented and validated in Eliseev et al. (2013).

Further, we present the equations of the model and validate the dynamical core using a parameter optimization experiment. Aeolus 1.0 is forced with prescribed surface temperature, surface humidity and cumulus cloud fraction to test the model's performance. In particular we examine the reproduction of the seasonal cycle and the influence of ENSO and compare relevant dynamical fields of the model output against seasonal means of ERA-Interim reanalysis data (climatology 1983-2009). The effects of parameter tuning are evaluated to improve the performance of the model.

In section 2 we present the novel equations of the Aeolus 1.0 dynamical core with the derivation of these equations presented in the ~~Suppl. Mat. .~~Supplementary Information (S1 – S2). The dynamical core is coupled with a convective plus 3-layer stratiform cloud scheme (which includes low-level, mid-level and upper-level stratiform clouds) developed by Eliseev et al. (2013). In section 3 we describe the experiment setup and the used reanalysis data sets. In section 4 we explain the model discretization and in section 5 we introduce our specific calibration method. For parameter optimization of the wind velocities we use Simulated Annealing which approximates the global minimum of a high-dimensional function ~~(Flechsig et al., 2013)~~(Flechsig et al., 2013). In section 6~~,~~ we present Aeolus' dynamical fields with pre-optimized and optimized parameters and compare them with observations and output from models of the Coupled ~~Climate Modeling Experiment~~Model Intercomparison Project Phase 5 (CMIP5). We conclude by discussing performance and limitations of the model in section 7.

Formatted: Font: Not Italic

Formatted: Font color: Black

2 Governing Equations

2.1 General structure of the atmosphere

~~*Aeolus* is a 2.5- dimensional statistical-dynamical model, with the vertical dimension largely parameterized and only coarsely resolved and it therefore belongs to the class of intermediate complexity atmosphere models. Water and energy conservations is achieved via a set of 2-dimensional, vertically averaged prognostic equations for temperature and water vapor (Petoukhov et al., 2000).~~

Aeolus 1.0 is a 2.5-dimensional SD model, with the vertical dimension being largely parameterized and only coarsely resolved and it therefore belongs to the class of intermediate complexity atmosphere models. Water and energy conservations is achieved via a set of 2-dimensional, vertically averaged prognostic equations for temperature and specific humidity (Petoukhov et al., 2000).

The 3-dimensional structure is described by these 2-dimensional surface fields with the vertical dimensions reconstructed using an equation for the lapse rate and assuming an exponential profile for specific humidity (Petoukhov et al., 2000).

For given temperature and specific humidity fields, the 3-dimensional wind field is calculated using a set of diagnostic equations. These statistical-dynamic equations for the wind fields are coupled and thus need several time steps or iterations to equilibrate.

The equations of the dynamical core of Aeolus describe the time evolution of1.0 are separated into equations for the (1) synoptic-scale transient waves (or storm tracks), (2) quasi-stationary planetary waves and (3) the zonal-mean wind. Thus, following classical statistical-dynamical approaches (Dobrovolski, 2000; Imkeller and von Storch, 2012)(Dobrovolski, 2000; Imkeller and von Storch, 2012), the key assumption is that the wind velocity field $\boldsymbol{V}V$ can be split into a synoptic scale $(\boldsymbol{V}')$ component V' (2-6 days period) and a large-scale long-term component $(\langle \boldsymbol{V} \rangle)\langle V \rangle$ (Fraedrich and Böttger, 1978) such that

$$\boldsymbol{V} = \langle \boldsymbol{V} \rangle + \boldsymbol{V}' = \{\langle \boldsymbol{u} \rangle, \langle \boldsymbol{v} \rangle, \langle \boldsymbol{w} \rangle\} + \{\boldsymbol{u}', \boldsymbol{v}', \boldsymbol{w}'\} V = \langle V \rangle + V' = \{\langle u \rangle, \langle v \rangle, \langle w \rangle\} + \{u', v', w'\} \quad (1)$$

The variables u, v and w describe the wind velocity in zonal, meridional and vertical direction. The brackets $\langle \dots \rangle(\langle \dots \rangle)$ symbolize time averaged quantities and the prime $(')(\dots')$ indicates deviations from this time averaged field. The large-scale long-term $\langle \boldsymbol{V} \rangle$component $\langle V \rangle$ is subdivided into a zonal-mean $\overline{\langle \boldsymbol{V} \rangle}$ $\overline{\langle V \rangle}$ and an azonal component $\langle \boldsymbol{V}^* \rangle \langle V^* \rangle$:

$$\langle \boldsymbol{V} \rangle = \overline{\langle \boldsymbol{V} \rangle} + \langle \boldsymbol{V}^* \rangle \langle V \rangle = \overline{\langle V \rangle} + \langle V^* \rangle \quad (2)$$

The large-scale, zonal-mean zonal wind velocity $\overline{\langle u(z,\phi) \rangle}$ with height above surface z and latitude ϕ is estimated using the generalassumed to be geostrophic (resulting in the thermal wind equation:balance):

$$\overline{\langle u(z,\phi) \rangle} = -\frac{1}{f}\left(\frac{1}{\rho_0}\langle \frac{\overline{\partial p_0}}{\partial \phi} \rangle + \int_0^z \frac{g}{T_0}\langle \frac{\overline{\partial T}}{\partial \phi} \rangle \, \mathrm{d}z\right) \frac{1}{a f}\left(\frac{1}{\rho_0}\langle \frac{\overline{\partial p_0}}{\partial \phi} \rangle + \int_0^z \frac{g}{T_0}\langle \frac{\overline{\partial T}}{\partial \phi} \rangle \, \mathrm{d}z\right), \quad (3)$$

whereby the sea level pressure gradient is calculated by $\langle \frac{\overline{\partial p_0}}{\partial \phi} \rangle = \frac{v^* \rho |f|}{-C_\alpha \sin \alpha}$ and α is the cross isobar angle defined as in Coumou et al. (2011). The variable v^* is the azonal meridional wind velocity, ρ is air density, f, the Coriolis parameter, reference air density ρ_0 and ϕ is the latitude. The Coriolis parameter f, reference air densitiy ρ_0, reference temperature T_0 and gravitational acceleration g (See Petoukhov et al., 2000).

where the sea level pressure gradient is calculated by $\langle \frac{\overline{\partial p_0}}{\partial \phi} \rangle = \frac{a v^* \rho |f|}{-C_\alpha \sin \alpha}$ with ageostrophic velocity parameter $C_\alpha = 5$ and the Earth radius a (derived and explained by Pethoukov et al. (2000), eq.(13)) and α is the cross-isobar angle defined as in Coumou et al. (2011), eq. (A31). The variable v^* is the azonal meridional wind velocity, ρ is the air density with the reference air density ρ_0, f the Coriolis parameter, ϕ is the latitude, T_0 is the reference temperature and g the gravitational acceleration (see Petoukhov et al., 2000).

As derived in S1.2the Suppl. Inf. in S2, the large-scale, zonal-mean meridional wind velocity $\overline{\langle v(z,\phi) \rangle}$ is given by

Formatted: Font: Not Italic

Formatted: Font: Not Bold

Formatted: Font: Not Bold

$$\overline{\langle v(z,\phi)\rangle} = \frac{d1*(-2\tan(\phi)\left(\overline{\langle u^*v^*\rangle}+\overline{\langle u'v'\rangle}\right))+d2*(\frac{\partial}{\partial\phi}\left(\overline{\langle u^*v^*\rangle}+\overline{\langle u'v'\rangle}\right))+d3*((\frac{z}{H_0}-1)\frac{\partial\overline{\langle u\rangle}}{\partial z}a)+d4*(A)}{n1*(\tan(\phi)\overline{\langle u\rangle})+n2*\left(-\frac{\partial\overline{\langle u\rangle}}{\partial\phi}\right)+n3*(2\Omega a\sin(\phi))}, \overline{\langle v(z,} \quad (4)$$

$$= \frac{d1*(-2\tan(\phi)\left(\overline{\langle u^*v^*\rangle}+\overline{\langle u'v'\rangle}\right))+d2*(\frac{\partial}{\partial\phi}\left(\overline{\langle u^*v^*\rangle}+\overline{\langle u'v'\rangle}\right))+d3*((-\frac{dK_z}{dz}+\frac{K_z}{H_0})\frac{\partial\overline{\langle u\rangle}}{\partial z}a)+d4*(A)}{n1*(\tan(\phi)\overline{\langle u\rangle})+n2*\left(-\frac{\partial\overline{\langle u\rangle}}{\partial\phi}\right)+n3*(2\Omega a\sin(\phi))},$$

Where d_1, d_2, d_3, d_4, n_1, n_2 and n_3 are tunable parameters and A represents the convection-related term

$$A = \frac{\mathcal{L}\overline{\langle P_{co}\rangle}}{H_0}\frac{\overline{\langle u_{sf}\rangle}}{\Gamma_a-\Gamma_0-\Gamma_1(T_a-T_0)(1-a_q q_s^2)+\Gamma_2 n_c}.$$

~~The vertical friction coefficient K_z, atmosphere scale height H_0, and Earth's angular velocity Ω as well as dry adiabatic lapse rate Γ_a, latent heat of evaporation $\mathcal{L}$ and model parameters Γ_0, Γ_1, Γ_2, a_q, T_0 are explained in **Table 1**. T_a is a temperature which would occur near the surface if the lapse rate did not change within the planetary boundary layer (PBL), q_s is the surface air specific humidity and n_c is the cumulus cloud amount. The variable $\overline{\langle P_{co}\rangle}$ is the convective precipitation rate and is calculated by the cloud model (Eliseev et al., 2013). The variable $\overline{\langle u_{sf}\rangle}$ is the surface wind and stated in the Supl. Ment. .~~

The atmospheric scale height H_0, the exchange for the momentums K_z, the the Earth's angular velocity Ω as well as the dry adiabatic lapse rate Γ_a, latent heat of evaporation $\mathcal{L}$ and model parameters Γ_0, Γ_1, Γ_2, a_q, T_0 are explained in **Table 1**. T_a is a temperature which would occur near the surface if the lapse rate did not change within the planetary boundary layer (PBL), q_s is the surface air specific humidity and n_c is the cumulus cloud amount. The latter variable is either computed by the cloud module or, as in this experiment, observational data is used. The variable P_{co} is the convective precipitation rate and is calculated by the cloud model (Eliseev et al., 2013). The variable u_{sf} is the zonal surface wind, see eq. (S10) in the Suppl. Information.

The azonal component of the large-scale wind field describes quasi-stationary planetary waves and depends on ~~the~~ latitude, longitude and height. At the equivalent barotropic level (EBL), azonal geostrophic components of horizontal velocities are computed employing the definition of the stream function ψ depending on latitude ϕ and longitude λ,

$$\langle u^*_{EBL}(\lambda,\phi)\rangle = -\nabla_\phi\frac{1}{a}\nabla_\phi\langle\psi^*_{EBL}\rangle \quad (5)$$

$$\langle v^*_{EBL}(\lambda,\phi)\rangle = \frac{1}{a}\nabla_\lambda\langle\psi^*_{EBL}\rangle \quad (6)$$

whereby the stream function can be subdivided into contributions from thermally and orographically induced waves depicted by subscript *th* and *or* respectively. They are considered to be additive due to linearity of the barotropic vorticity equations such that

$$\langle\psi^*_{EBL}\rangle = \Psi_0 \cdot \langle\psi^*_{th,EBL}\rangle + \langle\psi^*_{or,EBL}\rangle \quad (7)$$

The parameter Ψ_0 is a tuning parameter which is necessary since smoothing is applied to dampen local moisture feedbacks in the model. This smoothing however reduces spatial gradients in ψ^*_{EBL} and therefore u^*_{EBL} and ~~v^* itself~~v^*_{EBL} itself. The equation for the orographically induced waves is introduced in the Suppl. Inf. S1.2.

The zeroth order solution of the thermally induced waves of the barotropic vorticity equation is given by (see Suppl. ~~Information S.2~~Inf. S1.3.):

$$\langle\psi^*_{th,0,EBL}\rangle = -\langle T^*_{EBL}\rangle\frac{\cancel{a g}}{\cancel{\Omega\rho_0 T_0^2\cos\phi}}\frac{g}{\Omega\rho_0 T_0^2\cos\phi}\nabla_\phi\cancel{\int_0^{z_{EBL}}\rho_0\langle[T(z)]\rangle}\int_0^{z_{EBL}}\rho\langle[T(z)]\rangle\,dz \quad (8)$$

Formatted: English (U.S.)

Formatted: English (U.S.)

It is solved at two beta-planes, for the ~~northern~~Northern and ~~southern hemisphere~~Southern Hemisphere, respectively:

$$\langle\psi^*_{th,0,EBL}\rangle_{NH} = -\langle T^*_{EBL}\rangle\frac{\cancel{a g}}{\cancel{\Omega\rho_0 T_0^2\cos\beta_{NH}}}\frac{g}{\Omega\rho_0 T_0^2\cos\beta_{NH}}\nabla_\phi\cancel{\int_0^{z_{EBL}}\rho_0\langle[T(z)]\rangle}\int_0^{z_{EBL}}\rho\langle[T(z)]\rangle\,dz \quad (9)$$

$$\langle\psi^*_{th,0,EBL}\rangle_{SH} = -\langle T^*_{EBL}\rangle\frac{\cancel{a g}}{\cancel{\Omega\rho_0 T_0^2\cos\beta_{SH}}}\frac{g}{\Omega\rho_0 T_0^2\cos\beta_{SH}}\nabla_\phi\cancel{\int_0^{z_{EBL}}\rho_0\langle[T(z)]\rangle}\int_0^{z_{EBL}}\rho\langle[T(z)]\rangle\,dz \quad (10)$$

The beta-plane is an approximation, in which the Coriolis parameter is linearized to a reference latitude, ~~respectively~~ β_{NH} and β_{SH} for the Northern Hemisphere and Southern Hemisphere~~.~~, respectively. In the tropical belt the variable $\langle\psi^*_{th,0,EBL}\rangle$ is interpolated linearly between the two beta-planes

The standardized integrated heat content in equation (8) ($I_v = \cancel{\int_0^{z_{EBL}}\rho_0\langle[T^*(z)]\rangle}\int_0^{z_{EBL}}\rho\langle[T(z)]\rangle\,dz$) is calculated analytically by assuming a ~~constant~~ lapse rate $\Gamma = \Gamma_0 + \Gamma_1(T_a - T_0)(1 - a_q q_s^2) - \Gamma_2 n_c$ such that $T(z) = T(z_{EBL}) - \Gamma(z - z_{EBL})$. One obtains

$$I_v = \rho_0([T(z_{EBL})] - [\Gamma]z_{EBL})H_0\left(1 - e^{-\frac{z_{EBL}}{H_0}}\right) - \Gamma\rho_0 H_0\left\{(H_0 - z_{EBL})\left(e^{-\frac{z_{EBL}}{H_0}} - 1\right)\right\}$$

In addition, I_v is smoothed by ~~5~~five points in latitude to avoid numerical artefacts which may arise due to spatial differentiating.

To remove possible singularities near the poles, at high latitudes the stream function is dampened by a fourth order interpolation function. Planetary waves at other tropospheric ~~level~~levels are directly calculated from those at the EBL (see in the Suppl. ~~Mat.) .~~Inf. S1.1).

~~The~~Finally, the time averaged kinetic energy of transient eddies $\langle E'_k \rangle = \frac{1}{2}(\langle u'^2 \rangle + \langle v'^2 \rangle)$ is determined using the statistical-dynamical equations as described in Coumou et al., (2011)~~:~~

. Since detailed derivations are provided in Coumou et al. (2011), we only briefly discuss the diagnostic equations for transient eddy activity here. The equations are derived starting from the equation of the kinetic energy of transient eddies:

$$\frac{\partial \langle E'_k \rangle}{\partial t} = -\langle \boldsymbol{V} \rangle \cdot \nabla \langle E'_k \rangle + \langle u' \boldsymbol{V}' \rangle \cdot \nabla \langle u \rangle - \langle v' \boldsymbol{V}' \rangle \cdot \nabla \langle v \rangle + \sout{K_{fh} \nabla_H} K_{fh} \Delta_H \langle E'_k \rangle + K_{fz} \Delta_z \langle E'_k \rangle - K_{fs} \langle E'_k \rangle + f\left(\langle u' v'_{ag} \rangle - \langle v' u'_{ag} \rangle\right) \quad (11)$$

~~Here, K_{fh} and K_{fz} are internal atmospheric small/meso scale friction coefficients in the horizontal and vertical direction respectively, K_{fs} is the surface friction coefficient, f the Coriolis parameter and subscript "ag" denotes ageostrophic terms.~~

By assuming that the vertical (baroclinic) flux term is ~~equipartioned~~equipartitioned between the zonal and the meridional kinetic energy component, we can split ~~the~~ Eq. (~~9~~11) into three separate equations for $\langle u'^2 \rangle$,~~$\langle v'^2 \rangle$~~ $\langle v'^2 \rangle$ and $\langle u'v' \rangle$:

$$\frac{\partial \langle u'^2 \rangle}{\partial t} = -\langle \boldsymbol{V} \rangle \cdot \nabla \langle u'^2 \rangle - 2\langle u'^2 \rangle \frac{\partial \langle u \rangle}{\partial x} - 2\langle u'v' \rangle \frac{\partial \langle u \rangle}{\partial y} + K_{syn}\left[\left(\frac{\partial \langle u \rangle}{\partial z}\right)^2 + \left(\frac{\partial \langle v \rangle}{\partial z}\right)^2\right] + K_{fh}\Delta_H \langle u'^2 \rangle + K_{fz}\Delta_z \langle u'^2 \rangle - K_{fs}\langle u'^2 \rangle + f\left(\langle u' v'_{ag} \rangle - \langle v' u'_{ag} \rangle\right) \quad (12)$$

$$\frac{\partial \langle v'^2 \rangle}{\partial t} = -\langle \boldsymbol{V} \rangle \cdot \nabla \langle v'^2 \rangle - 2\langle v'^2 \rangle \frac{\partial \langle v \rangle}{\partial y} - 2\langle u'v' \rangle \frac{\partial \langle v \rangle}{\partial x} + K_{syn}\left[\left(\frac{\partial \langle u \rangle}{\partial z}\right)^2 + \left(\frac{\partial \langle v \rangle}{\partial z}\right)^2\right] + K_{fh}\Delta_H \langle v'^2 \rangle + K_{fz}\Delta_z \langle v'^2 \rangle - K_{fs}\langle u'^2 \rangle + f\left(\langle u' v'_{ag} \rangle - \langle v' u'_{ag} \rangle\right) \quad (13)$$

Formatted ...
Formatted ...
Formatted ...
Formatted Table
Formatted ...
Formatted: Font: 9 pt

$$\frac{\partial\langle u'v'\rangle}{\partial t} = -\langle \boldsymbol{V}\rangle\cdot\nabla\langle u'v'\rangle - \langle u'\boldsymbol{V}\rangle\cdot\nabla\langle v\rangle - \langle v'\boldsymbol{V}\rangle\cdot\nabla\langle u\rangle + K_{fh}\Delta_H\langle u'v'\rangle + K_{fz}\Delta_z\langle u'v'\rangle - K_{fs}\langle u'v'\rangle + f\left(\langle u'u'_{ag}\rangle - \langle v'uv'_{ag}\rangle\right)\left(\langle v'v'_{ag}\rangle - \langle u'u'_{ag}\rangle\right) \quad (14)$$

Here, K_{fh} and K_{fz} The parameterizations for K_{syn} and $f\left(\langle u'u'_{ag}\rangle - \langle v'uv'_{ag}\rangle\right)$ were found and derived in Coumou et al. are internal atmospheric small-/meso-scale friction coefficients in the horizontal and vertical direction respectively, K_{fs} is the surface friction coefficient, f the Coriolis parameter and the subscript "*ag*" denotes ageostrophic terms.

The terms for K_{syn}, the vertical macro-turbulent diffusion coefficient, and $f\left(\langle v'v'_{ag}\rangle - \langle u'u'_{ag}\rangle\right)$ need to be parameterized which is derived in Coumou et al. (2011). This way, a set of diagnostic equations for synoptic transient eddies is derived which, as also seen in equations (12) – (14), are all coupled to the large-scale wind field.

(2011).

This provides us with a coupled set of equations for $\overline{\langle u\rangle}, \overline{\langle v\rangle}, \langle u^*\rangle, \langle v^*\rangle, \langle u'^2\rangle, \langle v'^2\rangle$ and $\langle u'v'\rangle$, which can be solved. Cross terms like $\overline{\langle u^*v^*\rangle}$ can be determined by multiplying $\langle u^*\rangle$ with $\langle v^*\rangle$ and taking the zonal-mean of that quantity. All derivatives are determined numerically. The values of the parameters are listed in **Table 1**.

3 Forcing data and Reanalysis data sets

The simulations were forced by multi-year averages of monthly mean climatological, El Niño and La Niña months data (surface temperature, surface specific humidity, temperature at 500 mb500mb, geopotential height at 500 mb500mb and 1000 mb1000mb) using ERA-Interim Reanalysis Data (Dee et al., 2011) for 1983-2009 as our aim is that Aeolus captures year-to-year variability associated with the ENSO cycle. We identified 87 El Niño (74 La Niña) months using 3 month running meanmeans of ERSST. v4 SST anomalies (Huang et al., 2016) and applyingusing the definition that those months, where at least 5 consecutive overlapping seasons of SST anomalies are greater than 0.5K (less than -0.5K), are) for El Niño (La Niña) events.

Multi-year averages of monthly mean, El Niño and La Niña months cumulative cloud fraction is taken from ISSCP (Rossow and Commission, 1996). The spatial resolution is 2.5 × 2.5 degrees lat × lon and the time range is 1983-2009.

Multi-year averages of monthly mean, El Niño and La Niña months cumulative cloud fraction are taken from ISSCP (Rossow and Schiffer, 1999). The spatial resolution is 2.5 × 2.5 degrees lat × lon and the time range is 1983-2009.

We chose this time period, because the cumulative cloud fraction data is only available for this time period, which is needed to calculate the lapse rate is only available for this time period.

To avoid strong temperature gradients in the specified boundary conditions for the numerical experiments, we use the lapse rate equation to calculate temperatures at 1000 mb1000mb from those at 500 mb500mb. We first

Formatted ...

Formatted: Font: 9 pt

Formatted: Font: 9 pt

Formatted: Font: 9 pt, Not Bold, Font color: Auto

Formatted ...

Formatted: Font: Not Italic

calculate the lapse rate using the temperature field and specific humidity using the equation as given in Petoukhov et al. (2000) at ~~1000 mb~~1000mb. Then, we recalculate the temperature field at ~~1000 mb~~1000mb by using the temperature field at 500 mb and the linear lapse rate equation. This way we ensure that the temperature at ~~500 mb~~500mb is close to observations, and at the same time we have a vertical temperature ~~profile~~ realistic profile for a model like Aeolus. Since the ERA-Interim ~~500 mb~~500mb temperatures contain an orographic component, we exclude $\langle \psi^*_{or,EBL} \rangle$ in equation (7) in order not to incorporate orographic forcing of planetary waves twice.

We optimized the parameters for the numerical solutions of the wind velocities u^*, v^* and $\overline{\langle u \rangle}$ as well as eddy kinetic energy $\langle E'_k \rangle$ at ~~p = 500 mb~~500mb. To compare the strength and position of the Hadley and ~~Ferrel~~Ferrell cells between observation and model, we calculate a zonal-mean mass flux $\overline{\langle m \rangle}$ in the lower troposphere using the zonal-mean meridional wind velocity $\overline{\langle v \rangle}$ at levels between ~~1000 mb – 500 mb and~~1000mb–500mb, assuming exponential decay of air density with height ~~(Petoukhov et al., 2000)~~(Petoukhov et al., 2000).

For use with Aeolus, all data sets are interpolated to 3.75 × 3.75 degrees lat × lon spatial resolution.

4 Model discretization

Aeolus operates on a reduced grid to overcome the restriction of small time steps near the poles due to the CFL criteria (Jablonowski et al., 2009). In the grid generation, longitudinally adjacent cells are merged, if their zonal width in meters would be less than half of the cell width at the equator.

This way the reduced grid has the same resolution as a regular grid at the equator, but, at nominal resolution 3.75 × 3.75 degrees ~~lat × lon~~, around the poles only 6 cells are defined. On the regular grid, the maximum permissible time step due to the CFL criteria would be ~~ca~~approx. 5 min, while the limit for the reduced grid is ~~ca~~approx. 2 hours.

5 Calibration

The equations (1) – (14) are implemented in Aeolus and numerically solved on a 3.75 × 3.75 degrees ~~lat × lon~~ reduced grid with ~~5~~4 tropospheric height levels (~~1000 m, 3000 m, 5000 m, 9000 m~~1000m, 3000m, 5000m, 9000m).

Formatted: Font: Not Italic

The calibration of the winds is divided into two parts. First, we optimize the dynamical variables primarily driven by the thermal state of the atmosphere: The azonal velocities in zonal and meridional direction $\langle u^* \rangle$ and $\langle v^* \rangle$ as well as the zonal-mean zonal wind velocity $\overline{\langle u \rangle}$. In the second step, we tune the zonal-mean synoptic kinetic energy $\overline{\langle E'_k \rangle}$ and the lower troposphere integrated mass flux $\overline{\langle m \rangle}$, which solely ~~depends~~depend on the zonal-mean meridional wind $\overline{\langle v \rangle}$.

~~A common approach for parameter tuning is *Simulated Annealing* (Ingber, 1996) It is one experiment type in the multi-run simulation environment *SimEnv* for sensitivity and uncertainty analysis of model output (Flechsig et al., 2013) which we use for all calibration experiments.~~

~~For each model run, the thermal state of the atmosphere is kept constant (and initialized as described above) and the dynamical core is equilibrated to this thermal state. This typically requires only a few time steps. Since we~~

~~tune only the parameters of the dynamical core, Aeolus first calculates the clouds using its cloud scheme (Eliseev et al., 2013) to determine lapse rate and initialize the 3D thermal state. After that only the state of the dynamical core is updated.~~

A common approach for parameter tuning is Simulated Annealing (Ingber, 1996; Kirkpatrick, 1984). It is one experiment type in the multi-run simulation environment SimEnv for sensitivity and uncertainty analysis of model output (Flechsig et al., 2013) which we use for all calibration experiments. A schematic plot of the optimization process is shown in Suppl. Inf. S3.

For each model run, the thermal state of the atmosphere is kept constant (and initialized as described above) and the dynamical core is equilibrated to this thermal state. This typically requires only a few time steps. Since we tune only the parameters of the dynamical core, Aeolus first calculates the clouds using its cloud scheme (Eliseev et al., 2013) to determine the lapse rate and initialize the 3-dimensional thermal state. After that only the state of the dynamical core is updated each time step.

5.1 Dynamical ~~Core~~core Tuning - Step 1

For a good starting point the parameters are first tuned manually, providing "pre-~~optimised~~optimized" values. Next, we define physically realistic parameter- ranges for automatic tuning as listed in **Table 2**.

For the azonal wind velocities we use a weighting function which excludes the tropics (from 10°S to 10°N) and polar regions (poleward of 60°S for the Southern Hemisphere to exclude influences of Antarctica and poleward of 70°N for the Northern Hemisphere) such that the mid-latitudes, where planetary waves are important, are optimized.

The non-excluded grid as well as the zonal-mean zonal wind is weighted by $w(\phi) = |\cos(\phi)|$.

The total skill score for the scheme in step 1 is calculated by multiplying the individual skills for the azonal velocities in zonal and meridional direction (S_{u^*}, S_{v^*}) and the skill for the zonal-mean zonal wind velocity($S_{\overline{\langle u \rangle}}$):

$$S = S_{u^*} S_{v^*} S_{\overline{\langle u \rangle}}$$

The goal of the optimization procedure is to maximize the skill S.

Formatted: Font: Italic

Skill score functions for individual variables are computed as in Taylor (2001)

$$S(\phi, \lambda, t) = \frac{(1 + r_X)^4}{\left(A_X + {}^1/_{A_X}\right)^2} \quad (15)$$

In Eq. (~~15~~) r_X is the coefficient of the spatial correlation between the area-weighted modelled and observed fields of X; and A_X is the so-called relative spatial variation calculated according to

$$A_X = {}^{A_{X,M}}/_{A_{X,O}}. \quad (16)$$

Here, the variable ~~$\overline{A_{X,M}}$~~$A_{X,M}$ is the spatial average of $|X_M - X_{M,g}|$ and $X_{M,g}$ is a globally averaged value of the modelled field X_M. The observed field is similarly defined by ~~$\overline{A_{X,O}}$~~$A_{X,O}$.

5.2 Dynamical ~~Core~~core Tuning - Step 2

For tuning the zonal-mean meridional wind velocity $\overline{\langle v \rangle}$ and in particular the strength and width of the Hadley cell we use the vertical integral of the lower tropospheric integrated mass flux $\overline{\langle m \rangle}$. In addition, we tune the zonal-mean area-weighted synoptic kinetic energy $\langle E_k' \rangle$. Both variables strongly depend on the dynamic fields tuned in step 1, which is the reason for tuning them in a separate second step.

Total skill score for the scheme in step 2 is calculated by multiplying the individual skills for the vertical integral of lower troposphere mass flux ($S_{\overline{\langle m \rangle}}$) as well as the eddy kinetic energy ($S_{\langle E_k' \rangle}$)

$$S = S_{\overline{\langle m \rangle}} S_{\langle E_k' \rangle} S = S_{\overline{\langle m \rangle}} S_{\langle E_k' \rangle}$$

The goal of the optimization procedure is again to maximize skill S.

The skill score function for the eddy kinetic energy is given by the Taylor skill score function~~, e.g.~~ Eq. (15).

~~The skill score function for the mass flux consists of the product of the correlation of observation and model as well as the mean mass flux of the Hadley cell.~~ The skill score is then calculated by

$$S_{\overline{\langle m \rangle}} = \left(\text{mean}_{\text{Hadley\_Obs}} - \text{mean}_{\text{Hadley\_Model}}\right)^2 r_X^2 \qquad (17)$$

Here r_X is the coefficient of the spatial correlation between area-weighted modeled and observed fields (as in Eq. (15)), $\text{mean}_{\text{Hadley\_Model}}$ and $\text{mean}_{\text{Hadley\_Obs}}$ are the mean values of the area-weighted modeled and observed ~~fields.~~mean mass flux. We use this more elaborate skill function to promote a proper Hadley circulation in the model.

The weights of the lower troposphere mass flux $\overline{\langle m \rangle}$ are calculated according to:

$$w(\phi) = \begin{cases} |\cos(\phi)|, & \phi > 60°S \\ 0 & \phi \leq 60°S \end{cases} .$$

For calculating the mean intensity of the Hadley cell we determine the roots of the mass flux in observation data close to 0° and 30° which determine the Hadley cell latitudinal boundaries. This way, we have 36 values for the boundaries of the northern Hadley cell. Between these latitudinal borders we calculate the mean strength of the Hadley cell.

In **Table 3** the manually tuned (or pre-optimized) parameters and their ranges are listed.

6 Results

6.1 Results of Calibration – Step 1

We compared the numerical solutions using the optimized parameters for the wind fields $\langle u^* \rangle$, $\langle v^* \rangle$ and $\overline{\langle u \rangle}$ of climatological monthly averages, El Niño and La Niña months from ERA-Interim Reanalysis (Dee et al., 2011) for 1983-2009.

Formatted: Font: Italic

The figures for azonal wind velocities are divided into ~~6~~six subplots: The left column shows observational data and the right column model data. The top row shows climatological monthly averages, the middle multi-year averages of El Niño months and the bottom row multi-year averages of La Niña months.

In **Figure 1** and **Figure 2** the azonal component of the zonal wind ~~velocity~~velocities ($\langle u^* \rangle$) for February and August at ~~500 mb~~500mb are displayed, ~~–~~respectively. The figures show that with optimized parameters the model reasonably reproduces the main observed features both in terms of spatial position and magnitude. In particular the extra-tropical planetary waves are well captured with some minor discrepancies in the tropics. Both the seasonal cycle and the response to the ENSO cycle are well captured by the model.

Figure 3 and **Figure 4** show the same type of plots for ~~$\langle v^* \rangle$.~~the azonal meridional wind velocity ($\langle v^* \rangle$). Also for the meridional wind velocity the most important features of the reanalysis data are well represented in the model. The model results coincide well in wind strength and spatial pattern with the reanalysis data. The wind strength in winter, for both climatological and El Niño months are stronger than for ~~winter~~ La Niña months. In summer the opposite is seen for both model and reanalysis data.

In **Figure 5** the zonal-mean zonal wind velocity ~~$\overline{\langle u \rangle}$~~($\overline{\langle u \rangle}$) at ~~500 mb~~500mb is shown with the orange line representing reanalysis data, red representing model data with optimized parameters, and gray representing model data with pre-optimized parameters. The figure is subdivided into six subplots: The top row depicts $\overline{\langle u \rangle}$ in February and the bottom row shows $\overline{\langle u \rangle}$ in August ~~and~~, while the columns ~~providing respectively~~show climatological data, El Niño data and La Niña data~~.~~, respectively. It is noticeable that the results obtained with pre-optimized parameters are already reasonable ~~but that optimization hardly improves~~. Apparently the initial choice of tuning parameter values were already near the optimum and hence the optimized parameters lead only too small improvements of the model results. The Northern Hemisphere $\overline{\langle u \rangle}$ profile is well resolved in both seasons ~~and~~ for both El Niño and La Niña months. Parameter optimization slightly improves the results in the tropics. The modeled amplitude of $\overline{\langle u \rangle}$ in the Southern Hemisphere is too small in February for all plots, and too high in August ~~too high~~.

The optimized parameters are listed in **Table 2**. The β_{NH} in the Northern Hemisphere has a higher value, whereas the β_{SH} in the Southern Hemisphere has a lower value than the pre-optimized parameter values.

The last parameter is Ψ_0 and is changed to a higher value in order to strengthen ~~velocities~~speeds in $\langle v^* \rangle$ and $\langle u^* \rangle$.

6.2 Results of Calibration – Step 2

We compared the numerical solutions using the optimized parameters for the zonal-mean lower troposphere integrated mass flux $\overline{\langle m \rangle}$ and eddy kinetic energy $\overline{\langle E_K' \rangle}$.

The plots in ~~**Figure 6**~~**Figure 6** show that in general the monthly mean zonal-mean mass flux calculated with optimized parameters matches better with observational data. ~~The Hadley cell is generally too weak~~Here, the gain of the parameter optimization is clearly better than we saw with ~~pre-optimized parameters, which improves with the optimized parameters.~~calibration step 1. The ENSO cycle is clearly visible ~~and the width of the Hadley~~

~~cell is wider compared to results with pre-optimized parameters~~. However, the width of the Hadley cell (especially in August) is still too small compared to the width of the Hadley cell obtained by reanalysis data. The figure shows only plots with a latitudinal range from 60°S to 90°N as reanalysis data is spikey over Antarctica.

~~Figure 7~~Figure 7 shows the zonal-mean eddy kinetic energy $\overline{\langle E'_K \rangle}$. We show the same color code as in **Figure 6.** Northern Hemisphere modeled $\overline{\langle E'_K \rangle}$ profile is again well resolved in both seasons and for El Niño and La Niña months with the parameter optimization. Smaller spikes vanish such that the modeled $\overline{\langle E'_K \rangle}$ better matches the observed data. ~~However, the modeled optimized $\overline{\langle E'_K \rangle}$ curve in the Southern Hemisphere does not substantially improve compared to pre-optimized parameters.~~ The parameter optimization gained more improvement in NH than in SH.

In ~~Figure 8~~Figure 8 and **Figure 9** the eddy kinetic ~~energy $\overline{\langle E'_K \rangle}$~~energies $\langle E'_K \rangle$ for February and August ~~is~~are displayed. The left column shows observational data and the right column model data. The top row presents climatological monthly averages, the middle El Niño months and the bottom row La Niña months.

The spatial position and the magnitude are well captured, seasons and the ENSO-cycles are also well resolved, with some discrepancies in the tropics (i.e. the region over the Atlantic and Pacific Ocean) and the Southern Hemisphere. In February and August ~~$\overline{\langle E'_K \rangle}$~~$\langle E'_K \rangle$ is stronger ~~for both climatology and El Niño~~ in the Northern Hemisphere than in the Southern Hemisphere~~.~~ for both the climatology and in El Niño months. Only in La Niña months, ~~$\overline{\langle E'_K \rangle}$~~$\langle E'_K \rangle$ is weaker in the Northern Hemisphere.

The optimized parameters are listed in **Table 3**. The parameters ~~$U0$~~U_0 and m for optimizing the eddy kinetic energy are greater than the manually tuned values.

The parameters ~~$d3$~~d_3 and ~~$n3$~~n_3 are close to ~~one~~1, whereas the parameters ~~$d2, d4$~~d_2, d_4 and ~~$n1$~~n_1 are close to 2 and have a strong impact on the amplitude of the Hadley cell and the Ferrell cell. The parameter with the smallest influence is ~~$d1\ (d1 = 0.41).$~~d_1.

6.3 Comparison to CMIP5 Models

Figure 10 shows the comparison of February and August $\overline{\langle E'_K \rangle}$, $\overline{\langle u \rangle}$ and ~~$\overline{\langle m \rangle}$~~ $\overline{\langle m \rangle}$ between CMIP5 models (grey lines), Aeolus (red) and ERA-Interim data (orange). In General CMIP5 models represent the $\overline{\langle E'_K \rangle}$ and $\overline{\langle u \rangle}$ very well in both Hemispheres. However, in the Southern Hemisphere, the storm tracks, i.e. $\overline{\langle E'_K \rangle}$, of all models are too weak compared to observations with Aeolus on the lower end of the CMIP5 range. Further, some individual CMIP5 models can have too low or too high $\overline{\langle E'_K \rangle}$ and $\overline{\langle u \rangle}$ ~~as~~ compared to ERA~~—~~Interim, similar to Aeolus.

The CMIP5 multi-model mean of ~~$\overline{\langle m \rangle}$~~$\overline{\langle m \rangle}$ appears to be close to the reanalysis and most models reproduce this well. Still, some CMIP5 models can differ strongly from ~~$\overline{\langle m \rangle}$~~$\overline{\langle m \rangle}$ in ERA-Interim with some spikey behavior. Nevertheless, the width and strength of the Hadley cell is in most models well presented, but the Ferrell cell is often too strong. ~~Aeolus~~Aeolus' results give reasonable strength and width of the Ferrell cell, but the width of the Southern Hemisphere Hadley cell in August is too small compared to both reanalysis and CMIP5 models.

Formatted: Font color: Auto

Formatted: Font: Bold

7 Summary and Discussion

In this paper we presented the atmosphere model Aeolus, which is a ~~statistical-dynamical atmosphere model~~Statistical-Dynamical Atmosphere Model and belongs to the class of intermediate complexity models. The equations of Aeolus are time-averaged and the model has a spatial resolution of 3.75° × 3.75~~°~~.° degrees lat × lon. The 3-dimensional structure of Aeolus~~ is reconstructed using a set of 2-dimensional, vertically averaged prognostic equations for temperature and water vapor ~~(Petoukhov et al., 2000).~~ (Petoukhov et al., 2000). The advantage of such type of models is the fast computation time and for that reason the possibility to study and simulate long time periods as well as conduct sensitivity experiments.

We performed parameter optimization of the dynamical core consisting of a large multi-dimensional parameter space~~, which is in a high parameter range~~ and can be searched due to its fast computation time. For this approach we used the optimization algorithm Simulated Annealing, which approximates the global minimum of a high-dimensional function. We divided the calibration into two parts. ~~At first~~First, the azonal velocities in zonal and meridional direction as well as the zonal-mean zonal wind velocity were optimized, because they are primarily driven by the thermal state of the ~~atmospheres~~atmosphere. In the second step we optimized the zonal-mean synoptic kinetic energy and the lower troposphere integrated mass flux, and hence the zonal-mean meridional velocity, since those variables depend strongly on variables of step 1.

The results of the winds and eddy kinetic energy are in reasonable agreement with the reanalysis data and showed that our model is able to reproduce the dynamic response from the ~~season-~~seasonal cycle as well as the ENSO cycle which is a prime goal of our model development efforts. Parameter optimization in particular improves representation of the Hadley cell in terms of strength and width.

In the Southern Hemisphere the dynamical fields tend to be too weak. This model bias might be related to the missing ~~Antarctica~~Antarctic ice sheet, upper-tropospheric ozone, the constant lapse rate assumption, or fundamental limitations of the equations. These possibilities will be analysed in future work using the ~~coupled~~ Potsdam Earth Model (POEM) to which Aeolus has been coupled.

Compared to CMIP5 models, Aeolus reasonable well captures the dynamical state of the atmosphere in the Northern Hemisphere, particularly for monthly mean eddy kinetic energy $\overline{\langle E_K' \rangle}$, zonal-mean wind velocity $\overline{\langle u \rangle}$ and mass flux $\overline{\langle m \rangle}$. Especially the mass flux of the Ferrell cell is better captured than in other models, whereas the Southern Hemisphere Hadley cell width of Aeolus in August is too small compared to CMIP5 models.

8 Code and data availability

Code and data are stored in PIK's long term archive, and are made available to interested parties on request

9 Team list

S. Molnos, A. V. Eliseev, S. Petri, M. Flechsig, L. Caesar, V. Petoukhov and D. Coumou

Formatted: Font: Not Italic

Formatted: Font: Not Italic

Formatted: Font: Not Italic

Formatted: Font: Not Italic

10 Competing interests

The authors declare that they have no conflict of interest.

11 Acknowledgements

We thank ECMWF for making the ERA-Interim Data available.

The work was supported by the German Federal Ministry of Education and Research, grant no. 01LN1304A, (S.M., D.C.).

A.V.E. contribution was partly supported by supported by the Government of the Russian Federation (agreement No. 14.Z50.31.0033).

The authors gratefully acknowledge the European Regional Development Fund (ERDF), the German Federal Ministry of Education and Research and the Land Brandenburg for supporting this project by providing resources on the high performance computer system at the Potsdam Institute for Climate Impact Research.

12 References

Berger, A., Fichefet, T., Gallée, H., Tricot, C. and van Ypersele, J. P.: Entering the glaciation with a 2-D coupled climate model, Quat. Sci. Rev., 11(4), 481–493, doi:10.1016/0277-3791(92)90028-7, 1992.

Claussen, M., Mysak, L., Weaver, A., Crucifix, M., Fichefet, T., Loutre, M. F., Weber, S., Alcamo, J., Alexeev, V., Berger, A., Calov, R., Ganopolski, A., Goosse, H., Lohmann, G., Lunkeit, F., Mokhov, I., Petoukhov, V., Stone, P. and Wang, Z.: Earth system models of intermediate complexity: Closing the gap in the spectrum of climate system models, Clim. Dyn., 18(7), 579–586, doi:10.1007/s00382-001-0200-1, 2002.

Coumou, D., Petoukhov, V. and Eliseev, A. V.: Three-dimensional parameterizations of the synoptic scale kinetic energy and momentum flux in the Earth's atmosphere, Nonlinear Process. Geophys., 18(6), 807–827, doi:10.5194/npg-18-807-2011, 2011.

Dee, D. P., Uppala, S. M., Simmons, A. J., Berrisford, P., Poli, P., Kobayashi, S., Andrae, U., Balmaseda, M. A., Balsamo, G., Bauer, P., Bechtold, P., Beljaars, A. C. M., van de Berg, L., Bidlot, J., Bormann, N., Delsol, C., Dragani, R., Fuentes, M., Geer, A. J., Haimberger, L., Healy, S. B., Hersbach, H., Hólm, E. V., Isaksen, L., Kållberg, P., Köhler, M., Matricardi, M., Mcnally, A. P., Monge-Sanz, B. M., Morcrette, J. J., Park, B. K., Peubey, C., de Rosnay, P., Tavolato, C., Thépaut, J. N. and Vitart, F.: The ERA-Interim reanalysis: Configuration and performance of the data assimilation system, Q. J. R. Meteorol. Soc., 137(656), 553–597, doi:10.1002/qj.828, 2011.

Dobrovolski, S. G.: Stochastic Climate Theory~~,~~, Springer-Verlag Berlin Heidelberg, 2000.

Ehlers, E. and Krafft, T.: Understanding the Earth System: Compartments, Processes and Interactions, Springer-Verlag, Berlin, Heidelberg, 2001.

Eliseev, A. V., Coumou, D., Chernokulsky, A. V., Petoukhov, V. and Petri, S.: Scheme for calculation of multi-layer cloudiness and precipitation for climate models of intermediate complexity, Geosci. Model Dev., 6(5), 1745–1765, doi:10.5194/gmd-6-1745-2013, 2013.

Eliseev, A. V., Mokhov, I. I. and Chernokulsky, A. V.: An ensemble approach to simulate CO2 emissions from

natural fires, Biogeosciences, 11(12), 3205–3223, doi:10.5194/bg-11-3205-2014, 2014a.

Eliseev, A. V., Demchenko, P. F., Arzhanov, M. M. and Mokhov, I. I.: Transient hysteresis of near-surface permafrost response to external forcing, Clim. Dyn., 42(5–6), 1203–1215, doi:10.1007/s00382-013-1672-5, 2014b.

Flechsig, M., Böhm, U., Nocke, T. and Rachimow, C.: The Multi-Run Simulation Environment SimEnv~~, , 1,~~. [online] Available from: https://www.pik-potsdam.de/research/transdisciplinary-concepts-and-methods/tools/simenv/, 2013.

Fraedrich, K. and Böttger, H.: A Wavenumber-Frequency Analysis of the 500 mb Geopotential at 50° N, J. Atmos. Sci., 35(4), 745–750, doi:10.1175/1520-0469(1978)035<0745:AWFAOT>2.0.CO;2, 1978.

Ganopolski, ~~a~~A., Petoukhov, V., Rahmstorf, S., Brovkin, V., Claussen, M., Eliseev, ~~a~~A. V. and Kubatzki, C.: Climber-2: A climate system model of intermediate complexity. Part II: Model sensitivity, Clim. Dyn., 17, 735–751, doi:10.1007/s003820000144, 2001.

Harvey, L. D. D.: Milankovitch Forcing, Vegetation Feedback, and North Atlantic Deep-Water Formation, J. Clim., 2(8), 800–815, 1989.

Holland, M., Bitz, C., Eby, M. and Weaver, A.: The Role of Ice – Ocean Interactions in the Variability of the North Atlantic Thermohaline Circulation, J. Clim., 14, 656–675, doi:10.1175/1520-0442(2001)014<0656:TROIOI>2.0.CO;2, 2001.

Huang, B., Thorne, P. W., Smith, T. M., Liu, W., Lawrimore, J., Banzon, V. F., Zhang, H.-M., Peterson, T. C. and Menne, M.: Further Exploring and Quantifying Uncertainties for Extended Reconstructed Sea Surface Temperature (ERSST) Version 4 (v4), J. Clim., 29(9), 3119–3142, doi:10.1175/JCLI-D-15-0430.1, 2016.

Imkeller, P. and von Storch, J.-S.: Stochastic Climate Models, Birkhäuser~~.~~, 2012.

Ingber, L.: Adaptive simulated annealing (ASA): Lessons learned, Control Cybern., 25(1), 32–54, ~~doi:10.1.1.15.2777,~~ 1996.

Jablonowski, C., Oehmke, R. C. and Stout, Q. F.: Block-structured adaptive meshes and reduced grids for atmospheric general circulation models., Philos. Trans. A. Math. Phys. Eng. Sci., 367(1907), 4497–522, doi:10.1098/rsta.2009.0150, 2009.

Kirkpatrick, S.: Optimization by simulated annealing: Quantitative studies, J. Stat. Phys., 34, 975–986, doi:10.1007/BF01009452, 1984.

Knutti, R., Stocker, T. F., Joos, F. and Plattner, G.-K.: Constraints on radiative forcing and future climate change from observations and climate model ensembles, Nature, 416(6882), 719–723, doi:10.1038/416719a, 2002.

Latif, M.: Dynamics of interdecadal variability in coupled ocean-atmosphere models, J. Clim., 11(4), 602–624, doi:10.1175/1520-0442(1998)011<0602:DOIVIC>2.0.CO;2, 1998.

McGuffie, K. and Henderson-Sellers, A.: A Climate Modelling Primer, 3rd ed., J. Wiley and Sons, 2005.

Montoya, M., Griesel, A., Levermann, A., Mignot, J., Hofmann, M., Ganopolski, A. and Rahmstorf, S.: The

earth system model of intermediate complexity CLIMBER-3alpha. Part I: Description and performance for present-day conditions, Clim. Dyn., 25(2–3), 237–263, doi:10.1007/s00382-005-0044-1, 2005.

Petoukhov, V., Ganopolski, A., Brovkin, V., Claussen, M., Eliseev, A. V., Kubatzki, C. and Rahmstorf, S.: CLIMBER 2: a climate system model of intermediate complexity. Part I: model description and performance for present climate, Clim. Dyn., 16, 1–17, doi:10.1007/PL00007919, 2000.

Polyakov, I. V., Alekseev, G. V., Bekryaev, R. V., Bhatt, U. S., Colony, R., Johnson, M. A., Karklin, V. P., Walsh, D. and Yulin, A. V.: Long-term ice variability in Arctic marginal seas, J. Clim., 16(12), 2078–2085, doi:10.1175/1520-0442(2003)016<2078:LIVIAM>2.0.CO;2, 2003.

Rossow, W. B. and Schiffer, R. A.: Advances in Understandig Clouds from ISCCP, Bull. Amer. Meteor. Soc., 80(11), 2261–2287, doi:10.1175/1520-0477(1999)080<2261:AIUCFI>2.0.CO;2, 1999.

Saltzman, B.: A Survey of Statistical-Dynamical Models of the Terrestrial Climate, Adv. Geophys., 20(C), 183–304, doi:10.1016/S0065-2687(08)60324-6, 1978.

Schmittner, A. and Stocker, T. F.: The stability of the thermohaline circulation in global warming experiments, J. Clim., 12(4), 1117–1133, doi:10.1175/1520-0442(1999)012<1117:TSOTTC>2.0.CO;2, 1999.

Taylor, K. E.: Summarizing multiple aspects of model performance in a Single Diagram, J. Geophys. Res., 106(D7), 7183–7192, doi:10.1029/2000JD900719, 2001.

Xiao, X., Kicklighter, D. W., Melilo, J. M., McGuire, A. D., Stone, P. H. and Sokolov, A. P.: Linking a global terrestrial biogeochemcal model and a 2-dimensional climate model: implications for the global carbon budget, Tellus, 49B, 18–37, 1997.

Figures

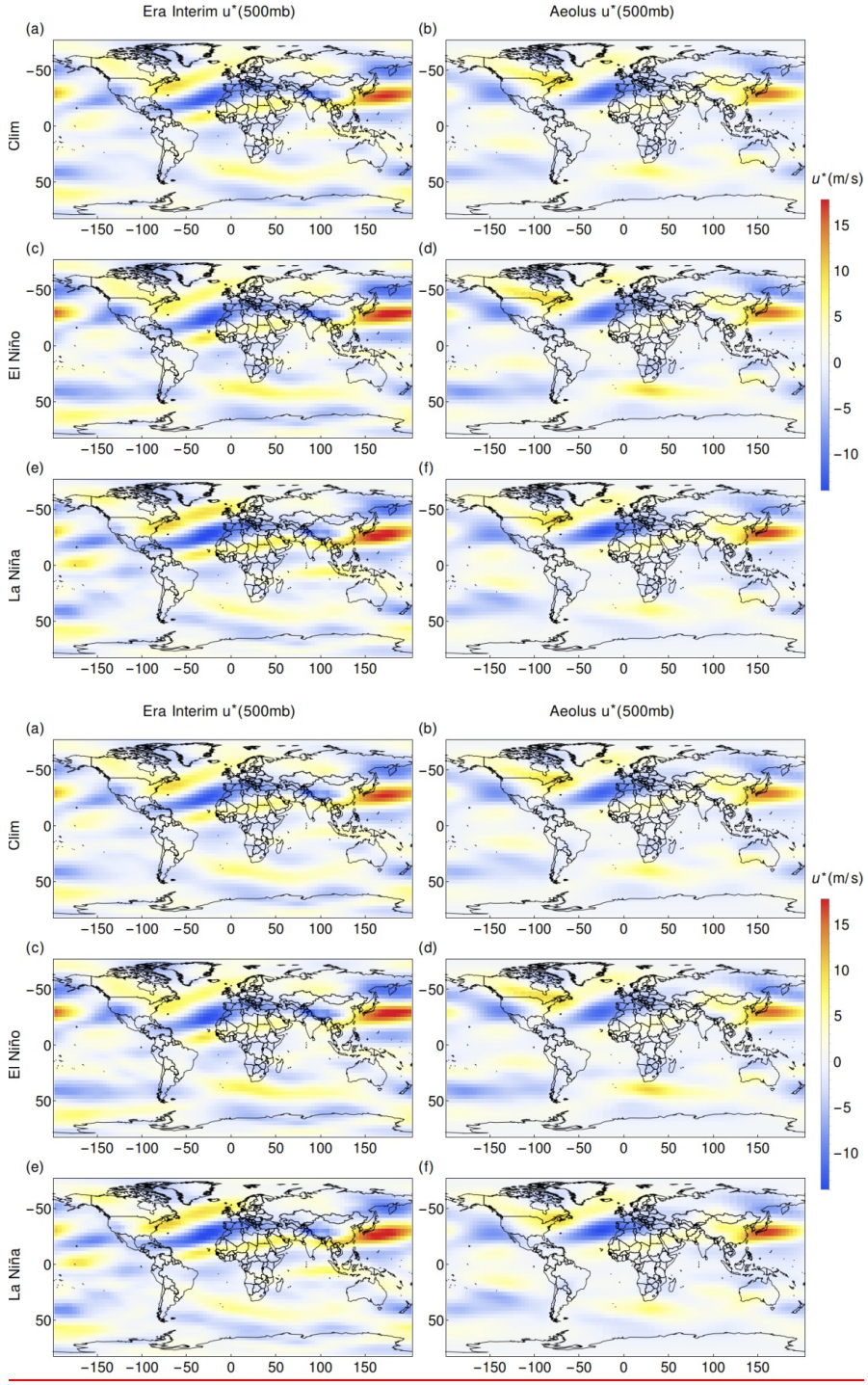

Era Interim u*(500mb)
Aeolus u*(500mb)
(a)
(b)
(c)
(d)
(e)
(f)
Clim
El Niño
La Niña
u*(m/s)
15
10
5
0
−5
−10
−150 −100 −50 0 50 100 150
−50
0
50

Figure 1 ~~**Monthly mean azonal**~~**Azonal large**~~**-**~~**-scale zonal wind u* ~~**in**~~**at 500mb for all February** ~~**at 500mb.**~~**months/ El Niño February months/ La Niña February months. The** ~~**first**~~**left column shows the results from** ~~**observation**~~**reanalysis data and** ~~**second**~~**the right column shows the results from Aeolus received by optimized parameters. The model is forced by surface temperature, humidity and cumulus cloud fraction.**

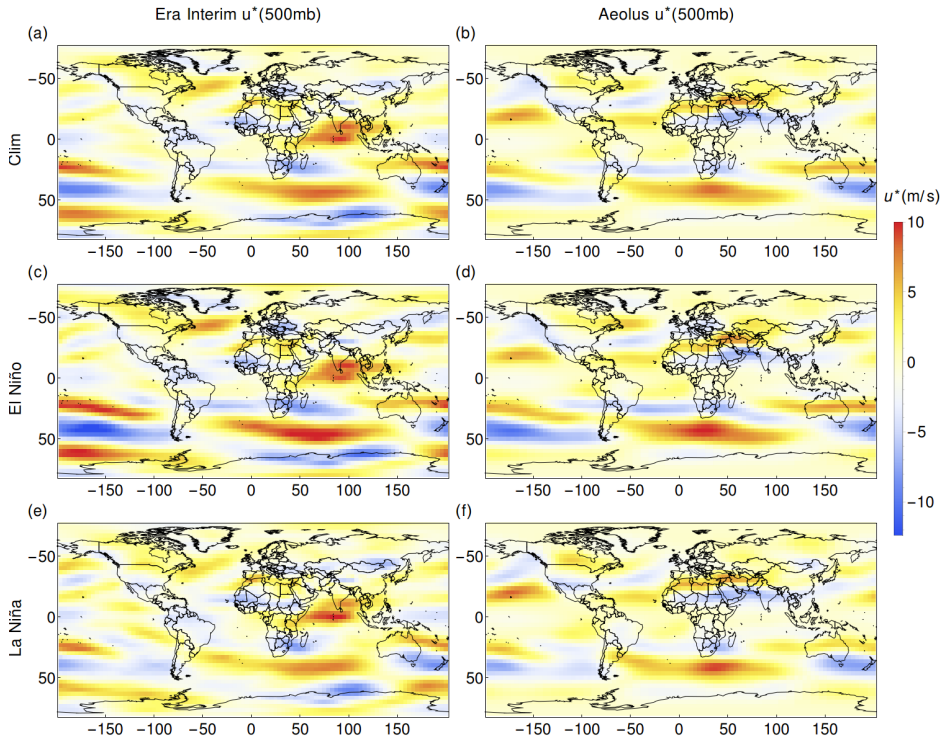

Figure 2 ~~**Monthly mean azonal**~~**Azonal large**~~**-**~~**-scale zonal wind velocity u* ~~**in August**~~ **at 500mb for August (compare Fig. 1).**

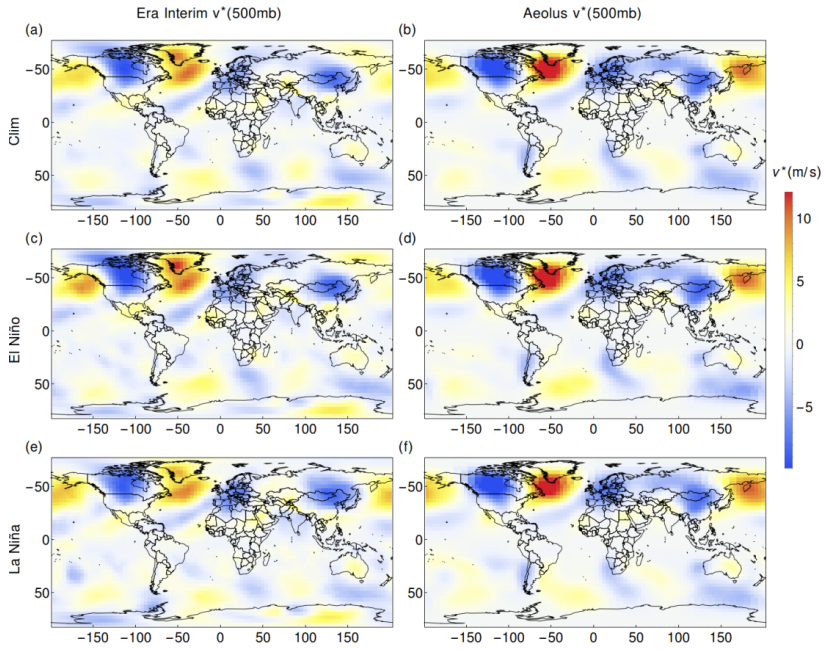

Figure 3 ~~Monthly mean azonal~~Azonal large ~~-~~scale meridional wind velocity v* ~~in February~~ at 500mb for February (compare Fig. 1).

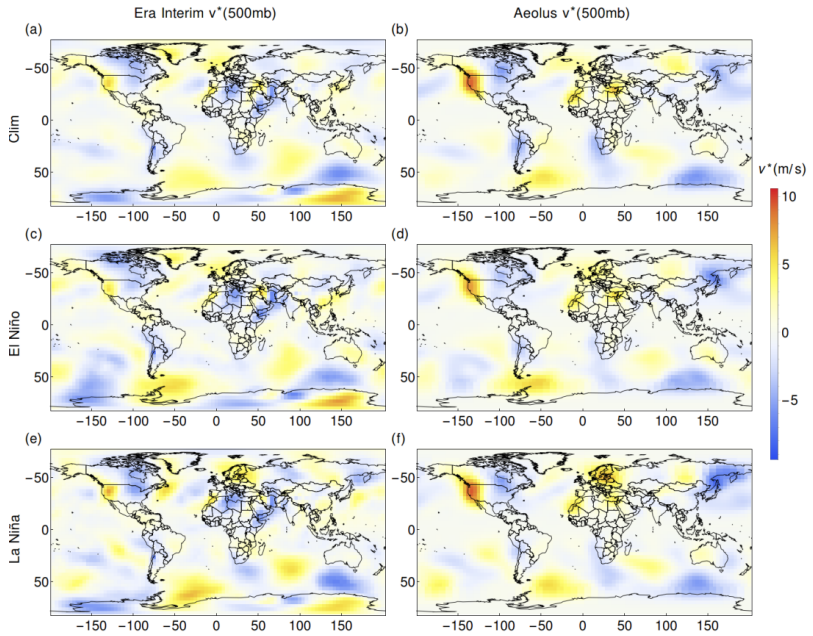

Figure 4 ~~Monthly mean azonal~~Azonal large ~~-~~scale meridional wind velocity v* ~~in August~~ at 500mb for August (compare Fig. 1).

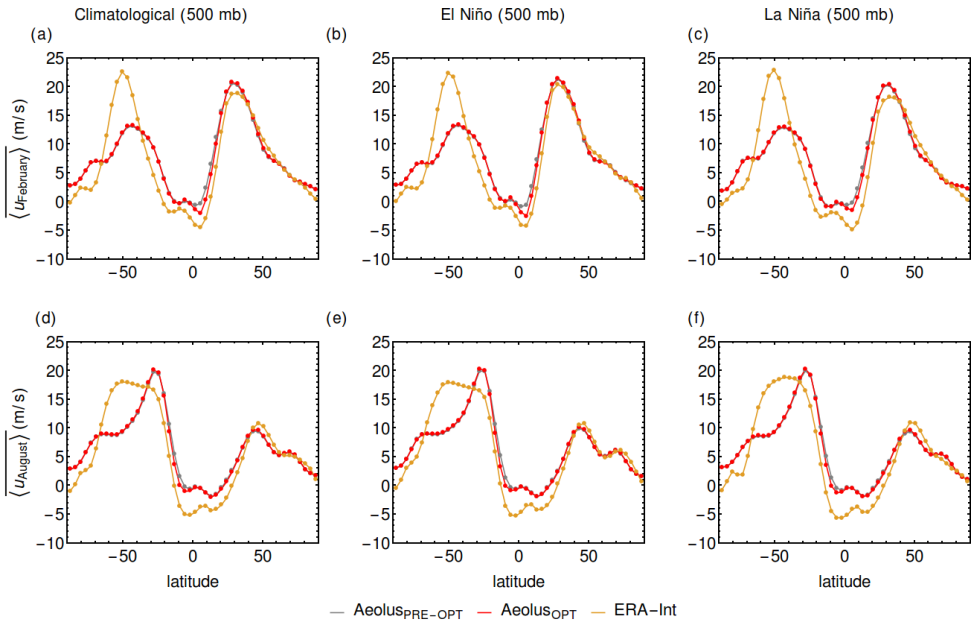

Figure 5 ~~**Monthly mean zonal**~~**Zonal-mean large-scale zonal wind velocity $\overline{\langle u(z,\phi)\rangle}$ at 500mb. (a) shows the** ~~**monthly mean**~~ **climatological monthly mean zonal-mean zonal velocity in February, (b) depicts the monthly mean zonal-mean velocity of** ~~**el niño months zonal-mean velocity in February**~~ **El Niño Februaries and (c) the monthly mean zonal-mean velocity of** ~~**el niña months zonal-mean velocity in February.**~~**La Niña Februaries. (d) displays the monthly mean climatological zonal-mean zonal velocity in August, (e) shows the monthly mean** ~~**of el niño months**~~ **zonal-mean velocity in** ~~**August and (f) the monthly mean of el niña months zonal-mean velocity in August.**~~**El Niño Augusts and (f) depicts the monthly mean zonal-mean velocity in La Niña Augusts. The yellow line represents zonal-mean large-scale zonal wind obtained by reanalysis data, the gray line is zonal-mean large-scale zonal wind velocity from Aeolus using pre-optimized parameters, and the red line represents zonal-mean large-scale zonal wind velocity from Aeolus using optimized parameters**

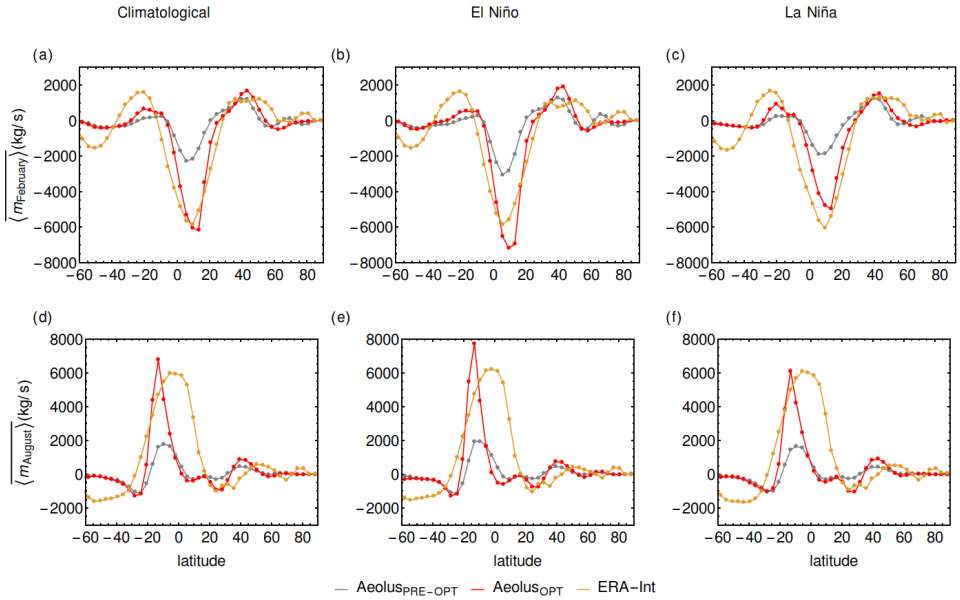

Figure 6 ~~Monthly mean zonal~~Zonal-mean large ~~-~~scale mass flux $\overline{\langle m \rangle}$. (a) shows the ~~monthly mean~~ climatological monthly mean zonal-mean mass flux in February, (b) depicts the monthly mean ~~of el niño months~~ zonal-mean mass flux ~~in February~~of El Niño Februaries and (c) the monthly mean ~~of el niña months~~ zonal-mean mass flux ~~in February.~~of La Niña Februaries. (d) displays the monthly mean climatological zonal-mean mass flux in August, (e) shows the monthly mean ~~of el niño months~~ zonal-mean mass flux in ~~August~~El Niño Augusts and (f) depicts the monthly mean ~~of el niña months~~zonal-mean mass flux in La Niña Augusts. The yellow line represents zonal-mean large scale mass flux obtained by reanalysis data, the gray line is the zonal-mean large scale mass flux from Aeolus using pre-optimized parameters, and the red line represents the zonal-mean large scale mass flux ~~in August~~from Aeolus using optimized parameters.

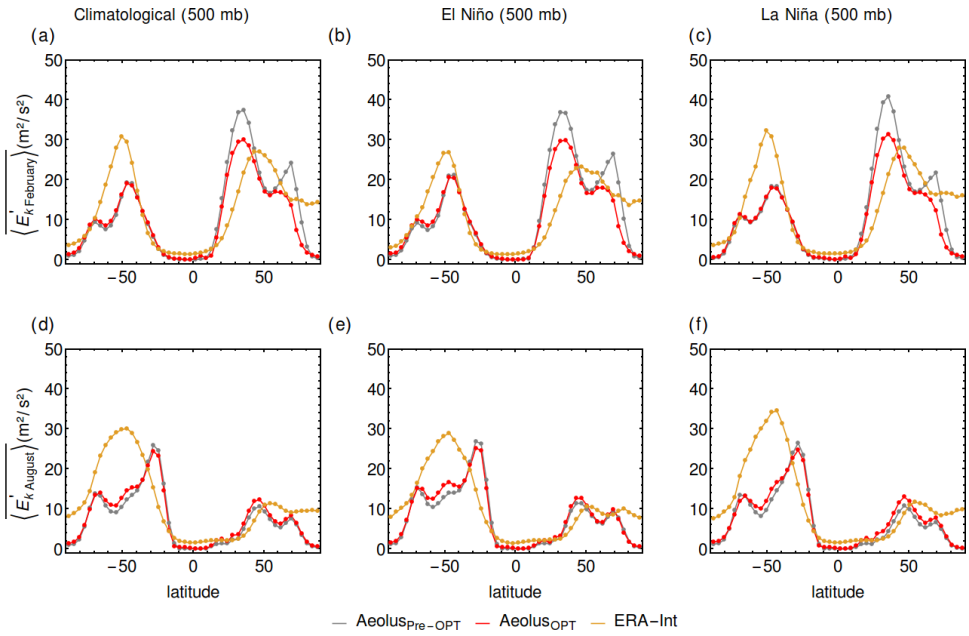

Figure 7 -Zonal-mean time averaged eddy kinetic energy $\overline{\langle E'_k \rangle}$ (compare Fig. ~~5~~6).

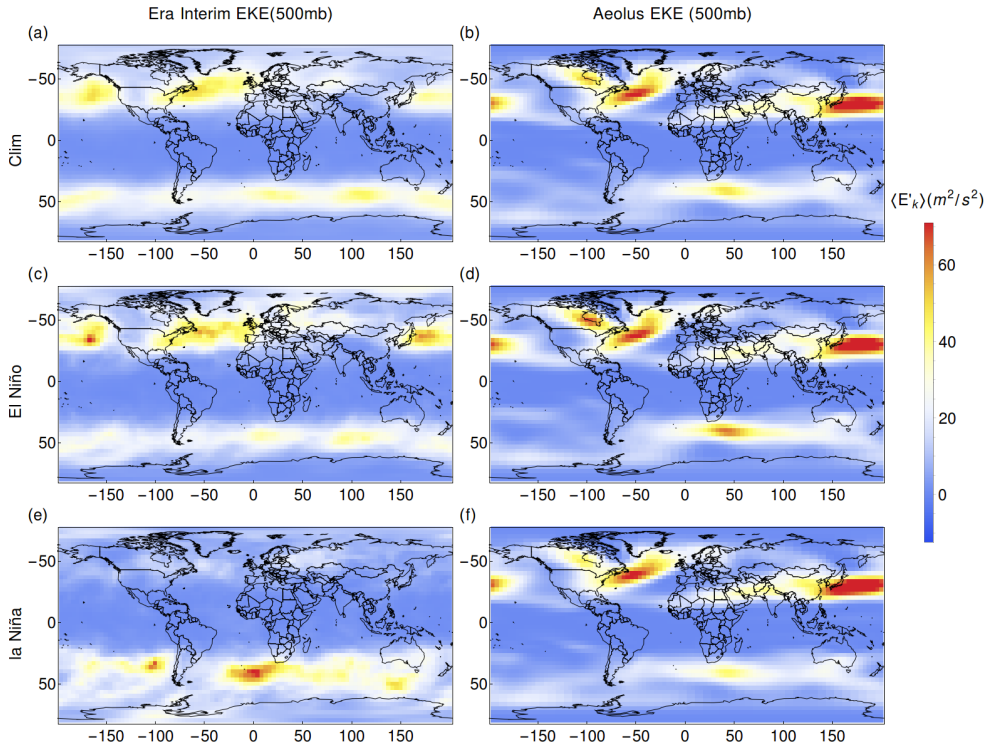

Figure 8 ~~Monthly mean time averaged eddy~~Eddy kinetic energy $\langle E_k' \rangle$ in February at 500mb (compare Fig. 1).

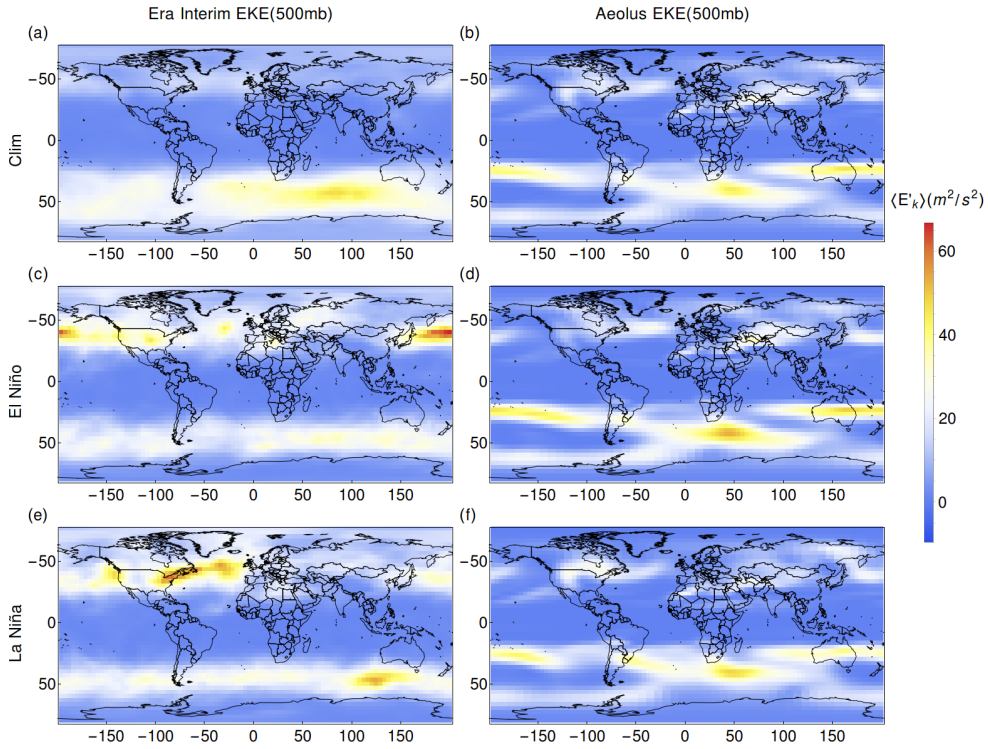

Figure 9 ~~Monthly mean time averaged eddy~~Eddy kinetic energy $\langle E_k' \rangle$ in August at 500mb (compare Fig. 1).

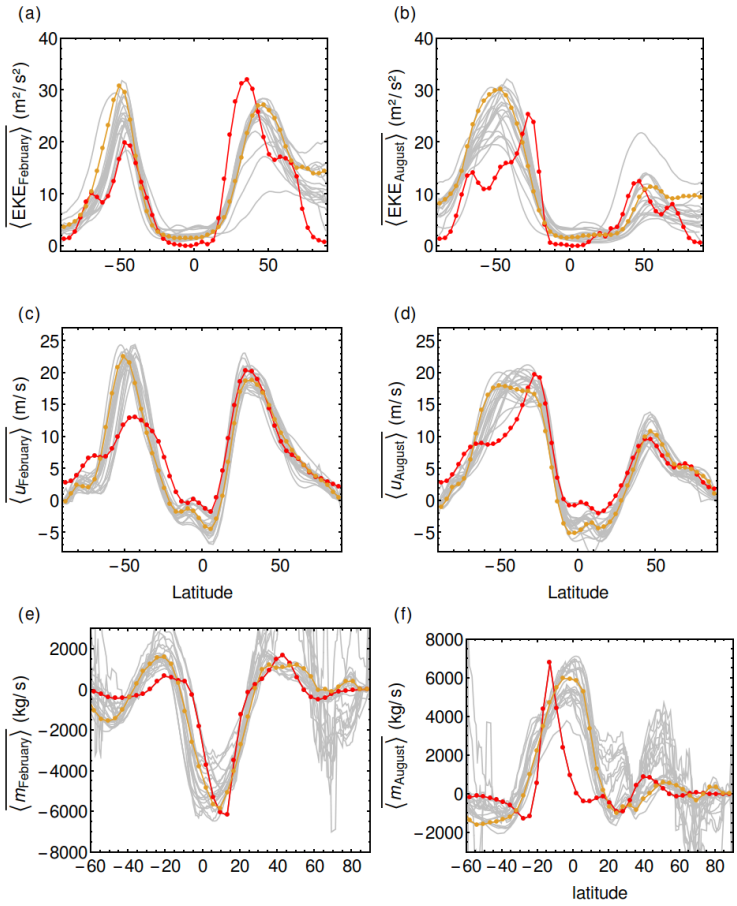
(a)
(b)
(c)
(d)
(e)
(f)
Latitude
Latitude
latitude

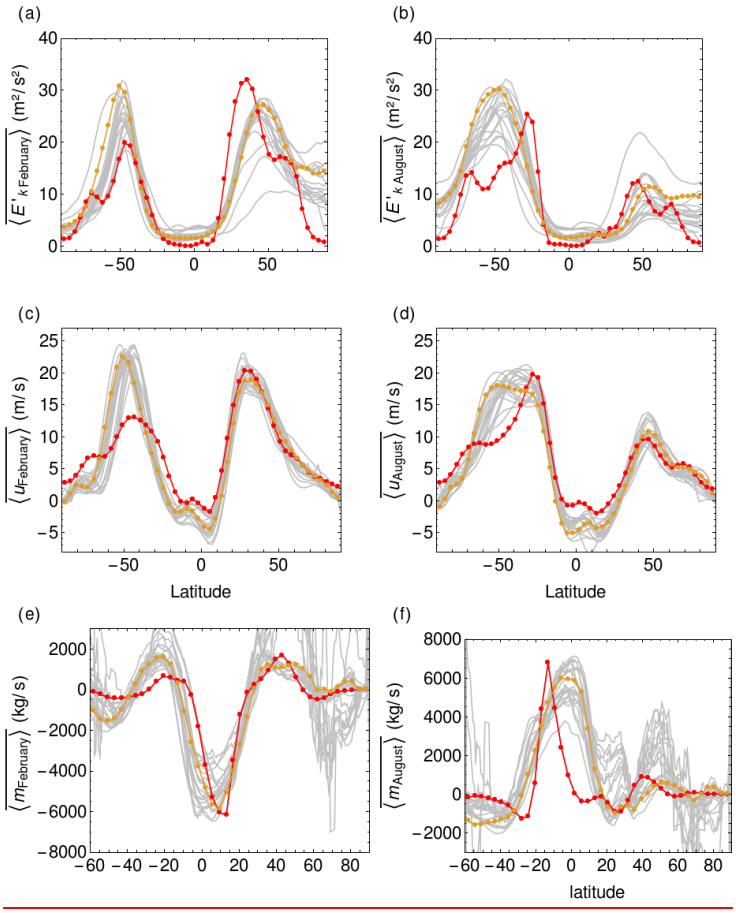

Figure 10 Comparison to CMIP5-Models. The orange line represents Era Interim data, the red line results from Aeolus, and grey lines CMIP5 Models (~~yearly~~annual mean zonal-mean data).

13 Tables

Table 1 Atmosphere model parameters

Symbol	Description	Value
a	Earth's radius	$6.4 \cdot 10^6$ m
ρ_0	Reference air density	1.3 kg m^{-3}
g	gravitational acceleration	9.8 ms^{-2}
T_0	Reference Temperature	273.16 K

f	Coriolis parameter	$2\Omega \sin(\phi)$
Ω	Earth's angular velocity	$7.3 \cdot 10^{-5} \mathrm{rad\ s^{-1}}$
C_α	Ageostrophic velocity parameter	5
α	cross-isobar angle	$\leq 10°$
H_0	Atmosphere scale height	$8 \cdot 10^3 \mathrm{m}$
L	Latent heat of evaporation	$2.257 \cdot 10^6 \frac{\mathrm{J}}{\mathrm{Kg}}$
Γ_a	Dry adiabatic Lapse Rate	$9.8 \cdot 10^{-3} \frac{\mathrm{K}}{\mathrm{m}}$
Γ_0	Temperature lapse rate ~~parameters~~parameter	$5.2 \cdot 10^{-3} \frac{\mathrm{K}}{\mathrm{m}}$
Γ_1	Temperature lapse rate parameter	$5.5 \cdot 10^{-5} \frac{1}{\mathrm{m}}$
Γ_2	Temperature lapse rate ~~parameters~~parameter	$10^{-3} \frac{\mathrm{K}}{\mathrm{m}}$
a_q	Temperature lapse rate ~~parameters~~parameter	$10^3 \left(\frac{\mathrm{kg}}{\mathrm{kg}}\right)^2$
K_z	coefficient of the small-scale and meso-scale turbulent exchange for the momentums	$0.005\ z\ \frac{m^2}{s}$

Table 2 Pre-optimized and optimized Parameter set and parameter ranges for optimization step 1

Parameters	Optimized value	Range	Pre-optimized value
ϕ_{flat0}	56.5	56.0:84.0	70.0
β_{NH}	57.2	30.0:60.0	37.5
β_{SH}	-31.3	-60.0:-30.0	-52.5
Ψ_0	10.14	7.4 : 12	8.0

Table 3 Pre-optimized and optimized Parameter set and parameter ranges for optimization step 2

Parameters	optimized value	Range	Pre-optimized value
U0	5.86	3.5:6.5	5
m	0.7849	0.4662:0.86658	0.6666
d1	0.41	0.:2.	1.0
d2	2.36	0.:2.5	1.0
d3	0.83	0.:2.5	1.0
d4	1.84	0.:2.5	1.0
n1	2.16	0.:2.5	1.0
n2	1.63	0.:2.	1.0
n3	1.06	0.:2.	0.5

Formatted: Font color: Background 1

Formatted: Font color: Background 1

S1 Supplementary Meterial Information

S1.1 Planetary Waves

The azonal component describes quasi stationary S1.1 Calculation of planetary waves. The calculation depends on the at tropospheric levels excluding EBL level of height.

At other tropospheric levels than the EBL, the equivalent barotropic level, azonal components of horizontal velocity are computed employing the definition of the stream functioncalculated by

$$\langle u^*_{EBL}(z)\rangle = -\nabla_\phi\langle\psi^*_{EBL}\rangle\langle u^*(z)\rangle = -\frac{1}{f\rho_0}\nabla_\phi\langle p^*_z\rangle \quad \text{(S1)}$$

$$\langle v^*_{EBL}(z)\rangle = \nabla_\lambda\langle\psi^*_{EBL}\rangle\langle v^*(z)\rangle = \frac{1}{f\rho_0}\nabla_\lambda\langle p^*_z\rangle, \quad \text{(S2)}$$

whereby theThe azonal component areis computed assuming isothermal expansion of air parcels in planetary waves

$$\langle p^*_z\rangle = \langle p^*_{EBL}\rangle\exp[(z-z_{EBL})/H_0] + \frac{p_* g}{\Gamma R}\exp[-z/H_0]\left\{\ln\left[\frac{T(z)}{T(z_{EBL})}\right] - \ln\left[\frac{\overline{T(z)}}{T(z_{EBL})}\right]\right\} \quad \text{(S3)}$$

and

$$\langle p^*_{EBL}\rangle = \rho\left\{\overline{\langle u_{EBL}\rangle}\right\}\nabla_\phi\langle\psi^*_{EBL}\rangle + 2\left(\frac{\overline{\langle u_{EBL}\rangle}}{a\cos(\phi)} + \Omega\right)\sin(\phi)\langle\psi^*_{EBL}\rangle \quad \text{(S4)}$$

S1.1.1 Planetary Waves – orographically2 Orographically induced stream function:

For the waves excited by the orography, the stream function is calculated by

$$\beta\nabla_\lambda\langle\psi^*_{or,0,EBL}\rangle = -\frac{f}{H_0}\langle w_{or}\rangle + \frac{f^2}{g}\frac{\partial\langle u'v'\rangle^*}{\partial z} \quad \text{(S5)}$$

Formatted: Header
Formatted
Formatted: Font: +Body (Calibri), 14 pt
Formatted: Font: +Body (Calibri), 14 pt
Formatted: Font: +Body (Calibri)
Formatted: Font: +Body (Calibri)
Formatted: Font: +Body (Calibri)
Formatted: Font: +Body (Calibri), Bold, English (U.K.)
Formatted: Font: +Body (Calibri), Bold
Formatted: Font: +Body (Calibri)
Formatted: Line spacing: Multiple 1,15 li
Formatted: Font: +Body (Calibri)
Formatted: Font: +Body (Calibri)
Formatted: Font: +Body (Calibri)
Formatted: Font: +Body (Calibri)
Formatted: Font: +Body (Calibri), English (U.S.)
Formatted: Font: +Body (Calibri)
Formatted: Line spacing: single
Formatted: Font: +Body (Calibri)
Formatted: Left, Line spacing: single
Formatted: Font: +Body (Calibri)
Formatted: Font: +Body (Calibri)
Formatted: Font: +Body (Calibri)
Formatted: Line spacing: single
Formatted: Font: +Body (Calibri), English (U.K.)
Formatted: Font: +Body (Calibri)
Formatted: Font: +Body (Calibri)
Formatted: Font: +Body (Calibri)
Formatted: Font: +Body (Calibri)
Formatted: Font: +Body (Calibri)
Formatted: Font: +Body (Calibri)
Formatted: Font: +Body (Calibri)
Formatted: Font: +Body (Calibri)
Formatted: Font: +Body (Calibri)
Formatted: Font: +Body (Calibri)
Formatted: Footer

where f is the Coriolis parameter and $\beta = \nabla_\phi f$ and

$$w_{or} = \langle u \rangle \nabla_\phi h_{or} + \langle v \rangle \nabla_\lambda h_{or} + a_{std}(\langle u \rangle^2 + \langle v \rangle^2 + \langle u'^2 \rangle + \langle v'^2 \rangle)^{1/2} h_{std} \quad \text{(S6)}$$

The variable h_{or} describes the grid cell averaged orography height h_{std} the subgrid scale standard deviation of the height of mountains, and a_{std} is an additional tuning parameter.

The azonal component describes quasi-stationary planetary waves and is subdivided into a geostrophic and ageostrophic term:

$$u^* = u^*_{geos} + u^*_{ageos}$$

$$v^* = v^*_{geos} + v^*_{ageos}$$

~~S1.2~~ S1.3 Zeroth order solution of the thermally induced waves of the barotropic vorticity equation at the EBL

We start from the z-projection of the baroclinic vorticity equation, which can be derived from the simplified Navier-Stokes-equation :

$$\bar{u}\frac{\partial}{\partial x}\left(\frac{\partial^2\langle\Psi^*_{EBL}\rangle}{\partial x^2}+\frac{\partial^2\langle\Psi^*_{EBL}\rangle}{\partial y^2}\right)+\beta\frac{\partial\langle\psi^*\rangle}{\partial x}=-\frac{\rho}{T_0}\frac{\partial\langle T^*_{EBL}\rangle}{\partial x}\frac{\partial\bar{p}}{\partial y}\frac{1}{{\rho_0}^2} \quad \text{(S7)}$$

with $\beta = \frac{2\Omega}{a}\cos\phi$, and Ω is the earth's rotation angular velocity, a is the earth's radius and ϕ the latitude.

In Eq. (S7) $\langle\Psi^*_{EBL}\rangle$ is the stream function of the azonal large-scale component at the equivalent barotropic level z_{EBL}, x and y are the horizontal and vertical direction, T_0 is the constant reference temperature and $\langle T^*_{EBL}\rangle$ is the large-scale long-term azonal temperature at the EBL. The variable $\bar{u}$ is the zonal mean zonal wind velocity, ρ_0 stands for the density near surface and $\bar{p}$ is the zonal mean pressure.

For the stream function of the azonal large-scale component of motion at the equivalent barotropic level z_{EBL} we use the ansatz

$$\langle\Psi^*_{EBL}\rangle = \langle\Psi^*_{0,EBL}\rangle + \epsilon\langle\Psi^*_{1,EBL}\rangle + \ldots$$

Formatted: Header
Formatted: Font: +Body (Calibri)
Formatted: Font: +Body (Calibri)
Formatted: Font: +Body (Calibri)
Formatted: Font: +Body (Calibri)
Formatted: Font: +Body (Calibri)
Formatted: Font: +Body (Calibri)
Formatted: Font: +Body (Calibri)
Formatted: Font: +Body (Calibri)
Formatted: Font: +Body (Calibri)
Formatted: Font: +Body (Calibri)
Formatted: Footer

For the zeroth order approximation, we can neglect higher order derivations of Ψ:

$$\beta \frac{\partial \langle \Psi^*_{0,EBL} \rangle}{\partial x} = -\frac{1}{\rho\, T_0} \frac{\partial \langle T^*_{EBL} \rangle}{\partial x} \frac{\partial}{\partial y} \frac{\int_0^\infty \rho \langle [T(z)] \rangle \, dz}{H_0} \qquad (S8)$$

In eq. (S8), we replaced $\bar{p} = \int_0^\infty R\rho\langle [T(z)] \rangle \, dz / H_0$ and $H_0 = RT_0/g$ and $\rho = \rho_0 \exp(-z/H_0)$, R is the gas constant, ρ is the air density, T is the temperature , H_0 is the atmospheric scale height, and g the gravity acceleration . Per definition, one can replace the term with

$$\frac{\int_0^\infty p \, dz}{H_0} = \frac{gR}{RT_0} 2 \int_0^{z_{EBL}} \rho \langle [T(z)] \rangle \, dz$$

Such that

$$\frac{\partial \langle \psi^*_{0,EBL} \rangle}{\partial x} = -\frac{agR}{2\Omega R T_0^2 \rho_0 \cos\phi} 2 \frac{\partial}{\partial y} \int_0^{z_{EBL}} \rho \langle [T(z)] \rangle \, dz \frac{\partial \langle T^*_{EBL} \rangle}{\partial x}$$

With latter equation and $\frac{1}{a} \nabla_\phi = \partial / \partial y$, we can then derive

$$\langle \psi^*_{0,EBL} \rangle = -\langle T^*_{EBL} \rangle \frac{g}{\Omega \rho_0 T_0^2 \cos\phi} \nabla_\phi \int_0^{z_{EBL}} \rho \langle [T(z)] \rangle \, dz$$

S2 Derivation of the zonal mean meridional wind velocity

The zonal mean meridional wind velocity $\langle \overline{v(z,\phi)} \rangle$ which also accounts for convective contribution is calculated by

$$\langle \overline{v(z,\phi)} \rangle = \frac{d1 * (-2\tan(\phi)\left(\overline{\langle u^* v^* \rangle} + \overline{\langle u' v' \rangle}\right)) + d2 * (\frac{\partial}{\partial \phi}\left(\overline{\langle u^* v^* \rangle} + \overline{\langle u' v' \rangle}\right)) + d3 * ((-\frac{dK_z}{z} + \frac{K_z}{H_0}) \frac{\partial \overline{\langle u \rangle}}{\partial z} a) + d4 * (A)}{n1 * (\tan(\phi)\overline{\langle u \rangle}) + n2 * \left(-\frac{\partial \overline{\langle u \rangle}}{\partial \phi}\right) + n3 * (2\Omega a \sin(\phi))} \qquad (S7S9)$$

With $K_z = 0.005\, z$ and ~~In (4)~~

~~$$A = \left(\frac{P_{conv}\, L}{(\Gamma_a - \Gamma)} - \frac{1}{H_0}\right) \langle u_{z\_profile} \rangle$$~~

Formatted: Header

Formatted: Font: +Body (Calibri)

Formatted: Font: +Body (Calibri)

Formatted: Font: +Body (Calibri)

Formatted: Font: +Body (Calibri)

Formatted: Font: +Body (Calibri)

Formatted: Footer

~~Whereby Γ is the lapse rate in the troposphere calculated by using the formula from Petoukhov (Petoukhov et al., 2000) , P_{conv} by the cloud module implemented by Eliseev at al. (Eliseev, n.d.) and~~

$$\langle u_{s\_profile} \rangle = \begin{cases} 2, & |\phi| > 40 \\ -2\cos\left(\phi \frac{\pi}{40°}\right), & \text{otherwise} \end{cases}$$

$$A = \frac{\mathcal{L}\langle P_{co} \rangle}{H_0} \frac{\langle u_{sf} \rangle}{\Gamma_a - \Gamma_0 - \Gamma_1 (T_a - T_0)\left(1 - a_q q_s^2\right) + \Gamma_2 n_c}$$

whereby the parameters are given in **Table 1**. We roughly approximate $\langle u_{sf} \rangle$ by constant profile for this experiment

$$\langle u_{sf} \rangle = \begin{cases} 2, & |\phi| > 40 \\ -2\cos\left(\phi \frac{\pi}{40°}\right), & \text{otherwise} \end{cases} \quad (S10)$$

The additional ~~calculating of $\langle u_{s\_profile} \rangle$~~calculation of $\langle u_{sf} \rangle$ instead of ~~using~~ the calculated surface zonal velocity is done to avoid instabilities. Instabilities can emerge due to the strong positive feedback between the meridional temperature and vertical wind velocity, which lead to high latent heat. In nature these would be damped out but due to fixed troposphere height, we parameterize it in the above described way.

For the derivation we start with the differential equation of the zonal wind component

$$\frac{du}{dt} = \frac{\tan\phi}{a} uv + fv - \frac{1}{\rho} \Delta_\lambda p + F_u \quad (~~S9~~ S11)$$

Whereby a is the Earth radius, f is the Coriolis factor and F_u is the frictional force in u-direction. Multiplying the equation with ρ and using that $\rho \frac{du}{dt} = \frac{d(\rho u)}{dt} - u\frac{d\rho}{dt}$, $\frac{d(\rho u)}{dt} = \frac{\partial(\rho u)}{\partial t} + \boldsymbol{V} \cdot \boldsymbol{\Delta}(\rho u)$ and $\boldsymbol{V} \cdot \boldsymbol{\Delta}(\rho u) = \Delta(~~\rho u \boldsymbol{V}~~)(\rho u \boldsymbol{V}) - (\rho u)\boldsymbol{\Delta} \cdot \boldsymbol{V}$, we get

$$\frac{\partial(\rho u)}{\partial t} + \Delta(\rho u \boldsymbol{V}) - u\left(\frac{d\rho}{dt} + (\rho u)\boldsymbol{\Delta} \cdot \boldsymbol{V}\right) = \frac{\tan\phi}{a} \rho uv + f\rho v - \Delta_\lambda p + \rho F_u$$

With the continuity equation and using spherical coordinates, the equation simplifies to

$$\frac{\partial(\rho u)}{\partial t} + \frac{1}{a\cos\phi}\frac{\partial(\rho u^2)}{\partial \lambda} + \frac{1}{a\cos\phi}\frac{\partial(\rho \cos\phi\, uv)}{\partial \phi} + \frac{\partial(\rho w u)}{\partial z} = \frac{\tan\phi}{a} \rho uv + f\rho v - \frac{1}{a\cos\phi}\frac{\partial p}{\partial \lambda} + \rho F_u \quad (S12)$$

Formatted: Header
Formatted: Font: +Body (Calibri)
Formatted: Font: +Body (Calibri)
Formatted: Font: +Body (Calibri)
Formatted: Font: +Body (Calibri)
Formatted: Font: +Body (Calibri)
Formatted: Font: +Body (Calibri)
Formatted: Font: +Body (Calibri)
Formatted: Font: +Body (Calibri)
Formatted: Font: +Body (Calibri)
Formatted: Font: +Body (Calibri)
Formatted: Font: +Body (Calibri)
Formatted: Font: +Body (Calibri)
Formatted: Position: Horizontal: Left, Relative to: Column, Vertical: In line, Relative to: Margin, Horizontal: 0 cm, Wrap Around
Formatted: Font: +Body (Calibri), German (Germany)
Formatted: Centered, Position: Horizontal: Left, Relative to: Column, Vertical: In line, Relative to: Margin, Horizontal: 0 cm, Wrap Around
Formatted Table
Formatted: Font: +Body (Calibri), Not Bold
Formatted: Footer

$$\frac{\partial(\rho u)}{\partial t} + \frac{1}{a\cos\phi}\frac{\partial(\rho u^2)}{\partial\lambda} + \frac{1}{a\cos\phi}\frac{\partial(\rho\cos\phi\, uv)}{\partial\phi} + \frac{\partial(\rho w u)}{\partial z} = \frac{\tan\phi}{a}\rho uv + f\rho v - \frac{1}{a\cos\phi}\frac{\partial p}{\partial\lambda} + \rho F_u \qquad (S10)$$

We calculate the zonal average $(\overline{\ldots})$, take into account that $\frac{\overline{\partial x}}{\partial\lambda} = 0$ and assume a vertical dependence of the density $(\rho = \rho_0(z))$ $(\rho = \rho_0(z))$:

$$\frac{\overline{\partial(\rho_0 u)}}{\partial t} + \frac{1}{a}\frac{\overline{\partial(\rho_0 uv)}}{\partial\phi} + \frac{\overline{\partial(\rho_0 wu)}}{\partial z} = 2\frac{\tan\phi}{a}\rho\overline{uv} + f\rho\bar{v} + \rho_0\bar{F}_u$$

We split the wind variables into an synoptic scale waves-, planetary waves and zonal mean wind ($u = \bar{u} + u^* + u'$) -'). Under the assumption that $\bar{u}$ and v^* are independent, the result of the zonal mean over the azonal component is zero:

$$\overline{uv} = \overline{\bar{u}\bar{v} + \bar{u}v^* + \bar{u}v' + u^*\bar{v} + u^*v^* + u^*v' + u'\bar{v} + u'v^* + u'v'}$$
$$= \overline{\bar{u}\bar{v} + \bar{u}v' + u^*v^* + u'\bar{v} + u'v'}$$

We average eq. (10) over time and phase speed (⟨…⟩). By assuming independency of the variables, we can simplify the terms $\langle\overline{\bar{u}v'}\rangle =$(S12) over time and phase speed (⟨… ⟩). Due to a "gap" in the three-dimensional (period-wavelength-phase velocity) spectrum of atmospheric processes (see, e.g., Fraedrich & Böttger 1978, Coumou et al. 2011), the synoptic-scale component in its interaction with the large-scale long-term component of the atmospheric fields on the time scales about 10-20 days and longer could be, to a first approximation, represented (described) in terms of its ensemble (statistical) characteristics (the second and higher-order moments), and not as the individual eddies (Saltzman, 1978). We can simplify the terms $\langle\overline{\bar{u}v'}\rangle = \langle\overline{u'\bar{v}}\rangle = 0$. In addition, it is $\overline{\bar{u}\bar{v}} = \bar{u}\bar{v}$ due to quasi stationarity of both terms. It is also $\langle\frac{dx}{dt}\rangle = 0$ and $\langle\bar{u}\bar{v}\rangle = \langle\bar{u}\rangle\langle\bar{v}\rangle$ since the oscillations of $\bar{u}$ and $\bar{v}$ are very small and independent of each other. By using the continuity equation $\frac{\rho_0}{a}\frac{\partial\langle\bar{v}\rangle}{\partial\phi} - \frac{\tan\phi}{a}\rho_0\bar{v} + \frac{\partial(\rho_0\langle\bar{w}\rangle)}{\partial z} = 0$, we can simplify -eq. (S10S12) to

$$\frac{1}{a}\rho_0\langle\bar{v}\rangle\frac{\partial\langle\bar{u}\rangle}{\partial\phi} + \frac{\rho_0}{a}\frac{\partial\left(\langle\overline{v^*u^*}\rangle + \langle\overline{v'u'}\rangle\right)}{\partial\phi} + \rho_0\langle\bar{w}\rangle\frac{\partial\langle\bar{u}\rangle}{\partial z} + \frac{\partial\left(\rho_0\langle\overline{w^*u^*}\rangle + \langle\overline{w'u'}\rangle\right)}{\partial z} = \frac{\tan\phi}{a}\rho_0\langle\bar{u}\rangle\langle\bar{v}\rangle + 2\frac{\tan\phi}{a}\left(\langle\overline{v^*u^*}\rangle + \langle\overline{v'u'}\rangle\right) + f\rho\bar{v} + \rho_0\bar{F}_u \qquad (S11 S13)$$

Formatted: Header
Formatted: Font: +Body (Calibri)
Formatted: Font: +Body (Calibri)
Formatted: Font: +Body (Calibri)
Formatted: Font: +Body (Calibri)
Formatted: Font: +Body (Calibri)
Formatted: Font: +Body (Calibri)
Formatted: Font: +Body (Calibri)
Formatted: Font: +Body (Calibri)
Formatted: Font: +Body (Calibri)
Formatted: Font: +Body (Calibri)
Formatted: Font: +Body (Calibri)
Formatted: Font: +Body (Calibri)
Formatted: Font: +Body (Calibri)
Formatted: Font: +Body (Calibri)
Formatted: Font: +Body (Calibri)
Formatted: Font: +Body (Calibri)
Formatted: Font: +Body (Calibri)
Formatted: Font: +Body (Calibri)
Formatted: Font: +Body (Calibri)
Formatted: Font: +Body (Calibri)
Formatted: Font: +Body (Calibri)
Formatted: Footer

With the assumption that $\rho_0 = e^{-z/H_0}$ and ~~$\rho_0\overline{F_u} = \frac{\partial\,\overline{\tau}}{\partial z} =$~~ $\frac{\partial}{\partial z}\left(\kappa\rho_0\frac{\partial\langle\overline{u}\rangle}{\partial z}\right) = \kappa\frac{\partial\rho_0}{\partial z}\frac{\partial\langle\overline{u}\rangle}{\partial z} + \rho_0\frac{\partial\kappa}{\partial z}\frac{\partial\langle\overline{u}\rangle}{\partial z} + \rho_0\kappa\frac{\partial^2\langle\overline{u}\rangle}{\partial z^2} = -\kappa\frac{\rho_0}{H_0}\frac{\partial\langle\overline{u}\rangle}{\partial z} + \rho_0\frac{\partial\kappa}{\partial z}\frac{\partial\langle\overline{u}\rangle}{\partial z}$~~, we obtain

$$\rho_0\langle\overline{v}\rangle\left(\frac{1}{a}\frac{\partial\langle\overline{u}\rangle}{\partial\phi} - \frac{\tan\phi}{a}\langle\overline{u}\rangle - f\right) = 2\frac{\tan\phi}{a}\left(\overline{\langle v^*u^*\rangle} + \overline{\langle v'u'\rangle}\right) - \frac{\rho_0}{a}\frac{\partial\left(\overline{\langle v^*u^*\rangle} + \overline{\langle v'u'\rangle}\right)}{\partial\phi} - \rho_0\langle\overline{w}\rangle\frac{\partial\langle\overline{u}\rangle}{\partial z} - \frac{\partial\left(\rho_0\overline{\langle w^*u^*\rangle} + \overline{\langle w'u'\rangle}\right)}{\partial z} - \kappa\frac{\rho_0}{H_0}\frac{\partial\langle\overline{u}\rangle}{\partial z} + \rho_0\frac{\partial\kappa}{\partial z}\frac{\partial\langle\overline{u}\rangle}{\partial z} \quad (\text{~~S12~~ S14})$$

The contribution to the vertical exchange of the atmospheric momentum from stationary eddies described in our case by zonally averaged $\overline{\langle w^*u^*\rangle}$ is shown negligibly small (Hantel and Hacker, 1978). ~~Also, the scale analysis attests that Also, the scale analysis attests that $\langle\overline{w}\rangle\frac{\partial\langle u\rangle}{\partial z}$ are small:~~Also, the scale analysis attests that $\langle\overline{w}\rangle\frac{\partial\langle u\rangle}{\partial z}$ are small (Petoukhov et al., 2003);

$$-\rho_0\langle\overline{w}\rangle\frac{\partial\langle\overline{u}\rangle}{\partial z} - \frac{\partial\left(\rho_0\overline{\langle w^*u^*\rangle} + \overline{\langle w'u'\rangle}\right)}{\partial z} - \kappa\frac{\rho_0}{H_0}\frac{\partial\langle\overline{u}\rangle}{\partial z} + \rho_0\frac{\partial\kappa}{\partial z}\frac{\partial\langle\overline{u}\rangle}{\partial z} \approx -\frac{\partial\left(\rho_0\overline{\langle w'u'\rangle}\right)}{\partial z} - \kappa\frac{\rho_0}{H_0}\frac{\partial\langle\overline{u}\rangle}{\partial z} + \rho_0\frac{\partial\kappa}{\partial z}\frac{\partial\langle\overline{u}\rangle}{\partial z}$$

Hence the eq. (~~S12~~S14) can be rewritten into

$$\rho_0\langle\overline{v}\rangle\left(\frac{1}{a}\frac{\partial\langle\overline{u}\rangle}{\partial\phi} - \frac{\tan\phi}{a}\langle\overline{u}\rangle - f\right) = 2\frac{\tan\phi}{a}\left(\overline{\langle v^*u^*\rangle} + \overline{\langle v'u'\rangle}\right) - \frac{\rho_0}{a}\frac{\partial\left(\overline{\langle v^*u^*\rangle} + \overline{\langle v'u'\rangle}\right)}{\partial\phi} - \rho_0\langle\overline{w}\rangle\frac{\partial\langle\overline{u}\rangle}{\partial z} - \frac{\partial\left(\rho_0\overline{\langle w^*u^*\rangle} + \overline{\langle w'u'\rangle}\right)}{\partial z} - \kappa\frac{\rho_0}{H_0}\frac{\partial\langle\overline{u}\rangle}{\partial z} + \rho_0\frac{\partial\kappa}{\partial z}\frac{\partial\langle\overline{u}\rangle}{\partial z} \quad (\text{~~S13~~ S15})$$

With $\langle\overline{u'w'}\rangle = -\kappa'\frac{\partial\langle\overline{u}\rangle}{\partial z}$, whereby ~~$\kappa'$~~ κ' is the coefficient of large-scale turbulent exchange for the momentum due to transient synoptic eddies ~~(Williams and Davies, 1965), we~~ (Williams and Davies, 1965), we get

$$\rho_0\langle\overline{v}\rangle\left(\frac{1}{a}\frac{\partial\langle\overline{u}\rangle}{\partial\phi} - \frac{\tan\phi}{a}\langle\overline{u}\rangle - f\right) = 2\frac{\tan\phi}{a}\left(\overline{\langle v^*u^*\rangle} + \overline{\langle v'u'\rangle}\right) - \frac{\rho_0}{a}\frac{\partial\left(\overline{\langle v^*u^*\rangle} + \overline{\langle v'u'\rangle}\right)}{\partial\phi} - (\kappa + \kappa')\frac{\rho_0}{H_0}\frac{\partial\langle\overline{u}\rangle}{\partial z} + \rho_0\frac{\partial(\kappa + \kappa')}{\partial z}\frac{\partial\langle\overline{u}\rangle}{\partial z}$$

With ~~$\tilde{\kappa} = \kappa + \kappa' K_z$~~ $\kappa + \kappa'$ we can simplify the equation to

$$\overline{\langle v(z,\phi)\rangle} = \frac{-2\tan(\phi)\left(\overline{\langle u^*v^*\rangle} + \overline{\langle u'v'\rangle}\right) + \frac{\partial}{\partial\phi}\left(\overline{\langle u^*v^*\rangle} + \overline{\langle u'v'\rangle}\right) + \left(-\frac{dK_z}{~~dz~~} + \frac{K_z}{H_0}\right)\frac{\partial\overline{\langle u\rangle}}{\partial z}a}{\tan(\phi)\overline{\langle u\rangle} - \frac{\partial\overline{\langle u\rangle}}{\partial\phi} + 2\Omega a\sin(\phi)}$$

Formatted: Header
Formatted ...
Formatted ...
Formatted ...
Formatted ...
Formatted: Font: 11 pt
Formatted ...
Formatted: Font: +Body (Calibri)
Formatted ...
Formatted: Font: +Body (Calibri)
Formatted: Font: +Body (Calibri)
Formatted ...
Formatted: Font: +Body (Calibri)
Formatted: Font: 10 pt
Formatted ...
Formatted ...
Formatted: Font: 11 pt
Formatted ...
Formatted ...
Formatted ...
Formatted ...
Formatted: Font: +Body (Calibri)
Formatted ...
Formatted ...
Formatted: Font: 10 pt
Formatted ...
Formatted: Font: +Body (Calibri)
Formatted: Font: +Body (Calibri)
Formatted: Footer

The derived equation for the meridional velocity does not account for latent heat release associated with convective precipitation. To capture this additional term we include convective precipitation and finally introduce tuning parameters, which have values close to 1.

S3 Schematic plot of the optimization process

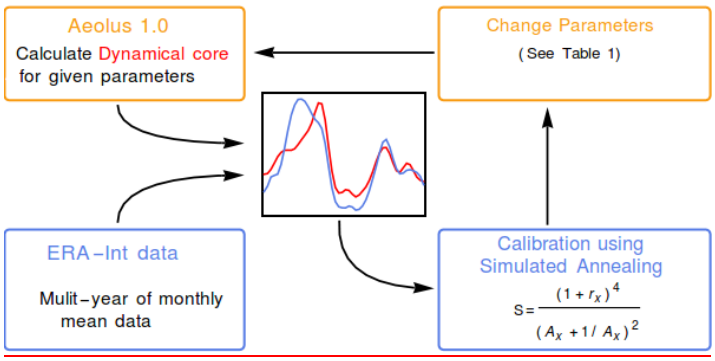

References

Hantel, M. and Hacker, J. M.: On the vertical eddy transports in the northern atmosphere. 1. Vertical eddy heat transport for summer and winter, J. Geophsical Res., 83, 1303–1318, 1978.

Petoukhov, V., Ganopolski, A. and Claussen, M.: POTSDAM - a set of atmosphere statistical-dynamical models: theoretical background, [online] Available from: https://www.pik-potsdam.de/research/publications/pikreports/.files/pr81.pdf, 2003.

Petoukhov, V., Rahmstorf, S., Petri, S. and Schellnhuber, H. J.: Quasiresonant amplification of planetary waves and recent Northern Hemisphere weather extremes, Proc. Natl. Acad. Sci. U. S. A., 110(14), 5336–5341, doi:10.1073/pnas.1222000110, 2013.

Saltzman, B.: A Survey of Statistical-Dynamical Models of the Terrestrial Climate, Adv. Geophys., 20(C), 183–304, doi:10.1016/S0065-2687(08)60324-6, 1978.

Williams, G. P. and Davies, D. R.: A mean motion model of the general circulation, Q. J. R. Meteorol. Soc., (January), 471–489, 1965.

Formatted: Header
Formatted: Font: +Body (Calibri)
Formatted: Font: +Body (Calibri)
Formatted Table
Formatted: Font: +Body (Calibri)
Formatted: Footer

(Petoukhov et al., 2013; Saltzman, 1978)

Formatted: Header

Formatted: Font: +Body (Calibri), Font color: Background 1

Formatted: Footer